A Biomechanical Simulation of Musculoskeletal Kinematics During Ambulation

Alex Thomas
Marquette University

A BIOMECHANICAL SIMULATION OF MUSCULOSKELETAL KINEMATICS
DURING AMBULATION

By

Alex Thomas, B.S.

A Thesis submitted to the Faculty of the Graduate School, Marquette University, in
Partial Fulfillment of the Requirements for the Degree of Master of Science

Milwaukee, Wisconsin

August 2018

ABSTRACT

A BIOMECHANICAL SIMULATION OF MUSCULOSKELETAL KINEMATICS
DURING AMBULATION

Alex Thomas, B.S.

Marquette University, 2018

The purpose of this study was to validate a 3D musculoskeletal model in OpenSim and assess OpenSim's ability to determine muscle-length variation during ambulation. An 18 camera motion capture system was used to analyze 20 healthy individuals between the ages of 18 and 35. Following data collection, the data was processed through OpenSim and Visual3D. The kinematic output processed through the OpenSim model was then compared to the kinematic output of the validated Visual3D model to validate the OpenSim model. Muscle fiber length data obtained from the same experimental data was compared to control data to assess OpenSim's muscle analysis functions. Spatiotemporal parameters including walking speed, left and right cadence, and stride length were also compared between the processed output from OpenSim and Visual3D. The mean maximum, minimum, and range of kinematics and muscle length data were calculated from the experimental and control data for comparison.

Paired t test statistical analysis was performed in comparing the right and left limb kinematics between OpenSim and Visual3D. One sample t test statistical analysis was performed in comparing the muscle-length output from the experimental and control data. Both statistical tests were conducted at a 95% confidence interval. The paired t test statistical analysis concluded varying results of significant similarities and differences at each joint during stance and swing phase between both sets of data. The one sample t test also resulted in varying results of significant similarities and differences for muscles in stance and swing phase between both sets of data.

OpenSim has variability in calculating inverse kinematics. Differences in the software compared to Visual3D support this claim. OpenSim's ability to calculate muscle-length changes sets it apart from Visual3D. The difference in anatomical modeling in OpenSim and Visual3D attributes to their difference in kinematic output. OpenSim's multitude of functions allows it to analyze different biomechanical aspects of human motion analysis. OpenSim's ability to determine inverse kinematics and muscle-length variation during gait can ultimately help physicians, biomedical engineers and clinicians to further assess motion analysis and properly prescribe restorative surgeries and therapies.

ACKNOWLEDGMENTS

Alex Thomas, B.S.

I would like to thank my mother, father, grandmother, and two brothers for all the support they have given me during my graduate career. Their encouragement and support have helped me on countless occasions. They continue to inspire me in all aspects of life and have taught me to put my full effort into everything I do. They played a key role in inspiring me to pursue further education within the field of biomedical engineering. My family comes from a very religious background, and I am so thankful that they have instilled in me a solid faith in God. I would not be where I am today if it were for my loved ones, my faith, and God.

I would also like to thank everyone in my committee, Dr. Gerald Harris, Dr. Jacob Rammer, and Dr. Kruger for always being so extremely helpful throughout my graduate career from the very beginning. They have always provided excellent advice when it comes not only to my graduate schooling and research but also advice in future aspirations. Dr. Tina Garman has also been of great help throughout my research development. Despite living across the country with a full-time job and family, she has found time to help me with troubleshooting many different parts of my project on numerous occasions. I also want to thank Cheryl Wanta for helping me coordinate meetings and ensuring I met approaching deadlines well in advance. I appreciate everything this group of individuals has done for me.

LIST OF CONTENTS

LIST OF TABLES

LIST OF FIGURES

I.   INTRODUCTION

A. Definition of Motion Analysis

Motion analysis plays an essential role within the realm of rehabilitation engineering. Motion analysis can be defined as a technique used by clinicians to quantify human movement patterns. Clinicians can then analyze these movement patterns with biomechanical software and assess any inconsistencies or discrepancies shown in the data. Gait analysis is a branch of motion analysis focusing primarily on the lower extremities during ambulation. It is used in pretreatment assessment, surgical decision making, postoperative follow-up, and management of both adult and younger patients [1]. Gait abnormalities include deviations at multiple joints in multiple planes of motion (3 planes of a Cartesian coordinate system). Looking at the lower extremities, gait deviations can be prevalent at the trunk, hip, knee, and ankle. Some examples of gait abnormalities resulting from deviations at the hip include Trendelenburg gait, scissoring, and circumduction. Such resulting from deviations at the knee includes stiff knee gait, flexed knee gait, and recurvatum. And those resulting from deviations at the ankle include dropfoot and toe-toe gait [2]. Gait deviations are commonly seen in the pediatric population. Gait analysis is useful in understanding the disturbances in gait patterns seen in children and adolescents with cerebral palsy. It has also helped better scientifically and clinically evaluate how orthopaedic surgical procedures modify gait [3]. Therefore it is clear that clinical gait analysis is an important measure necessary in identifying, assessing, and correcting gait.

B. Marker Sets

An automated tracking system gives the most in-depth and sophisticated analysis for gait. These systems utilize either active or passive markers in order to track motion. Active markers are optoelectric meaning they are actively illuminated and are tracked that way within the motion capture volume. LEDs are most commonly used. Active markers give users the opportunity to capture motion at higher sampling rates. Active marker based models often use a larger number of markers than passive marker based systems. One limitation with these markers is that subjects must wear power packs consisting of an electronic circuit and batteries. This complicates the building of markers/tracking targets [4].

Like active markers, passive markers require much data processing through algorithms via computer coding to identify the center marker position to optimize tracking. Passive markers are not luminescent like active markers however they are often retro-reflective. Passive markers are beamed with light of a spectrum mostly lower than the light spectrum perceivable by the naked eye. Cameras used in motion analysis are equipped with a filter that recognizes this spectrum associated with these markers. As a result passive markers appear as bright spots in the images produced by the cameras.

Several different marker sets have been created and validated for use in motion analysis. The purpose of placing markers on anatomic landmarks of the body is to better capture motion. More markers may be placed on a specific segment if there is a focus on analyzing motion of that particular segment in one or more planes. Markers are generally placed on bony prominences of the body to ensure the least amount of noise due to skin and tissue artifact. During gait analysis each camera surrounding the motion capture

volume is capable of capturing a 2D view of each marker, but in order to determine the markers' 3D coordinates each marker must be visible by at least two cameras. Therefore multiple cameras are often times used in motion analysis to ensure the 3D position of each marker can be determined.

As mentioned earlier, more markers can be placed on a particular segment if there is inherent noise present or if the segment is complex, meaning lots of room for movement/different joints within the segment. The foot is a great example of a complex segment. The Milwaukee Foot Model Marker Set includes 12 markers on each foot as shown in Figure 1.

Milwaukee Foot Model Marker Set

Marker Number	Marker Name	Description
1	MSAT	Medial superior anterior tibia
2	MMAL	Medial malleolus
3	LMAL	Lateral malleolus
4	TCAL	Calcaneal tuberosity
5	MCAL	Medial calcaneus
6	LCAL	Lateral calcaneus
7	T5ML	Tuberosity of the 5th metatarsal laterally
8	MH1M	Medial Head of the 1st metatarsal
9	LH5M	Lateral head of the 5th metatarsal
10	XHAL	Hallux triad x-axis
11	YHAL	Hallux triad y-axis
12	ZHAL	Hallux triad z-axis

Figure 1: Milwaukee Foot Model marker set [5].

The foot can be broken down into multiple segments. The marker-based segmental definition of the foot includes four separate segments including the tibia, hindfoot, forefoot, and hallux. There is more motion at the foot since there are many different bones and joints within the foot. This validated marker set is able to accurately

describe motion at the foot in all three planes due to the amount of markers and their precise placement [6].This is also the reason why knee alignment devices are used (KAD) since the knee is a complex joint and has many ligaments and tissues within it.

Kainz et al. [7] conducted an experiment to test the reliability of four biomechanical models for clinical gait analysis. Two of the models were analyzed through Direct Kinematics for joint kinematic calculations, whereas the other two musculoskeletal models, mainly used for research, were analyzed through Inverse Kinematics. Direct kinematics is defined as a method to calculate joint kinematics as the Cardan angles between adjacent segments which are defined from rigid 3D marker locations. Inverse kinematics on the other hand is defined as a method to calculate joint kinematics by adjusting a skeletal-joint model with markers rigidly attached such that the model's joint angles attain the best match between virtual and experimental marker positions. All four models however exhibited the same marker set for motion tracking. The marker set can be seen in Figure 2.

Abbreviation	Placement/Full name	Model			
		PiG-DK	6-DoF-DK	3-1-1-DoF-IK	3-3-2-DoF-IK
RASI/LASI	anterior superior iliac spine	A, T	A, T	A, T	A, T
RPSI/LPSI	posterior superior iliac spine	A, T	A, T	A, T	A, T
RTHI/LTHI	thigh wand marker	T	-	-	-
RTH1/LTH1	thigh cluster marker 1	-	T	T	T
RTH2/LTH2	thigh cluster marker 2	-	T	T	T
RTH3/LTH3	thigh cluster marker 3	-	T	T	T
RKNE/LKNE	lateral knee	A, T	A	A, T	A, T
RMKNE/LMKNE	medial knee	A	A	A	A
RTIB/LTIB	shank wand marker	T	-	-	-
RTB1/LTB1	shank cluster marker 1	-	T	T	T
RTB2/LTB2	shank cluster marker 2	-	T	T	T
RTB3/LB3	shank cluster marker 3	-	T	T	T
RANK/LANK	lateral ankle	A, T	A	A, T	A, T
RMMA/LMMA	medial malleolus	A	A	A	A
RTOE/LTOE	Top of the second metatarsal head	A, T	A, T	A, T	A, T
RD5M/LD5M	Lateral at the head of the 5th metatarsal	-	A, T	A, T	A, T
RHEE/LHEE	Posterior aspect of the heel	A, T	A, T	A, T	A, T

Figure 2: Marker set used in *Kainz et al.*

As seen in Figure 2 there is a marker cluster both at the thigh and shank segments. The distance between markers on the long axis of the clusters was 10.5 cm and the third marker of the clusters was orthogonal to the long axis 4.5 cm from the midpoint. The thigh cluster is placed on the lateral distal thigh and the shank cluster is placed on the medial distal shank. More markers are placed here due to the larger amount of adipose tissue on these segments. Markers sticking out on wands can help with tracking rotational movement. The thigh and shank have more adipose tissues surrounding them than the locations of the other markers such as the anterior superior iliac spine, knee, and ankle/foot. Another marker set that utilizes clusters of markers is known as the Cleveland Clinic Model. This model is based around a cluster of markers on a rigid base attached to each segment [8], but unfortunately the documentation of this marker set is very poor within scientific literature.

C. Biomechanical Models

The Conventional Gait Model, also known as the Plug-in Gait Model, is distinct in that it is known for its simplicity in marker placement. Subsequently this marker set can be used from young to old populations   in gait analysis. Figure 3 displays the marker set used in the Conventional Gait Model which is known as the Helen-Hayes marker set. There are markers placed on the anterior superior iliac spine, two on the posterior superior iliac spine, the thigh, knee, shank, lateral malleolus, calcaneus, and second metatarsal head. There are two variations of the Helen-Hayes marker set. They are different in that one variation uses two posterior superior iliac spine markers, (PSIS_R and PSIS_L) and another variation that simply uses one posterior superior iliac spine marker.
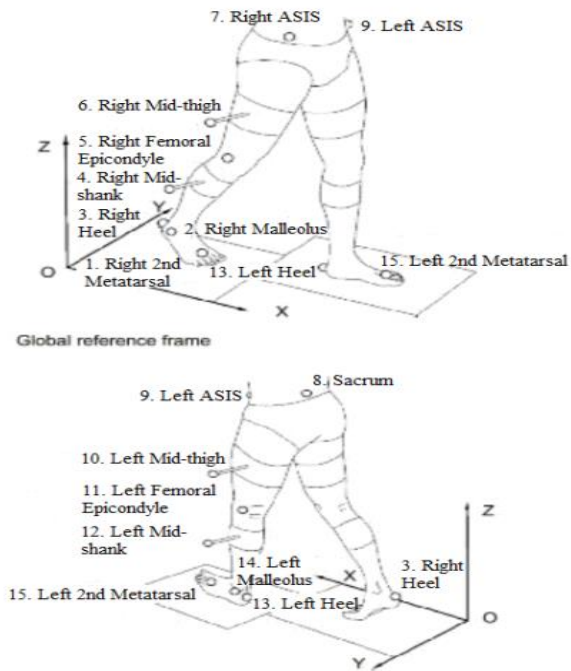
Figure 3: Helen-Hayes marker set [9].

Once a marker set has been established, it must be coupled with a biomechanical model. A biomechanical model can be created with biomechanical analysis software such as Visual3D, OpenSim, Nexus, etc. with an applied marker set. Modern gait analysis requires a biomechanical model to infer the positions of body segments from the measured positions of markers placed on the subject [10].

Kainz et al. [7] analyzes four different biomechanical models in his article titled *Reliability of four models for clinical gait analysis.* Two of the models being analyzed through Direct Kinematics (DK) and the other two are musculoskeletal models being analyzed through Inverse kinematics (IK). One of the two DK models is the Vicon Plug-in-Gait model. DK was used to calculate joint kinematics and output three rotations at the pelvis, hip, and knee joints and two rotations at the ankle joint. The pelvic marker

locations and the leg length measure defined the hip joint center. One static and one walking trial were collected and processed in order to evaluate the knee profile rather than using a KAD (in accordance with standard clinical practices at Queensland Children's Motion Analysis Laboratory). The other DK model had 6 degrees of freedom which was created by Vicon Motion Systems' BodyBuilder software.

D. Available Motion Capture Systems

There are plenty of different motion capture systems currently being used to analyze human motion. Vicon is one of the leading developers in motion capture products. Vicon uses different software as biomechanical analysis tools including Shogun, Nexus, Tracker, and Blade. This software is optimal for different types of motion analysis whether it be sports biomechanics, gait biomechanics, etc. For example Nexus software is data capture software for clinical, biomechanics and sports science customers. Tracker software is used for fast, precise object tracking and can be done with a single camera.

Optitrack is another leading developer in motion capture systems. They not only provide motion analysis software and high-speed tracking cameras, they also offer contract engineering services. Big companies like Nike brand and Mayo Clinic use Optitrack motion capture systems in gait analysis and movement sciences. They use Motive: Body as production motion capture software. This software provides one-click subject calibration, precision finger tracking, expanded subject counts, and kinematic labeling. Motive supports several different marker sets even if the model was created through different software. An Optitrack motion analysis system is used in this study in conjunction with Visual3D and AMASS software.

Motion Analysis Corporation (MAC) also plays a huge role within the motion analysis industry. They have produced multiple different motion capture systems and software. Notable camera systems include their line of Kestrel and Raptor cameras. Different software is used for different applications including baseball swing analysis, drone tracking, rearfoot motion analysis, gait analysis, golf swing analysis, etc. But the most popular motion analysis software they use is called Cortex which encompasses all the aspects of data analysis, from calibration to post-processing and is capable of calculating kinematics, kinetics, and muscle data via EMG. MAC has also supports software to analyze muscle dynamics called SIMM, which was created by MusculoGraphics. SIMM can be used with any gait analysis software and is capable of computing muscle moment arms and changes in muscle lengths during gait.

Qualisys is another company specializing in motion capture based in Sweden. They are a leading provider of precision motion capture and 3D positioning tracking systems for multiple fields including engineering, biomechanics, virtual reality, robotics, and movement sciences. They provide motion analysis solutions in all conditions whether it be indoor, outdoor or under water. They provide a wide range of motion analysis products including cameras, EMG, force plates, eye tracking, and open sound control. Qualisys uses Visual3D biomechanical software to conduct gait analysis.

E. Practical Applications

Gait analysis is especially useful within the realm of rehabilitation. Gait abnormalities can be very complicated and can involve several muscles and joints of the lower extremities in multiple planes of motion. Clinical tests can be performed for several

reasons including to determine a diagnosis between disease entities, assessment of the severity, extent or nature of a disease or injury, monitoring progress in the presence or absence of intervention, and prediction of the outcome of intervention [8]. Richard Baker proposed that criterion used to perform clinical tests can be modified to fit the criterion for performing clinical gait analysis, which includes reasons like distinguishing diagnosis between disease entities, to determine severity of a disease or injury, to select among treatment options, predicting prognoses, etc [8]. Gait deviations can stem anywhere from muscle weakness, abnormal muscle tone, static or dynamic muscle contracture, to abnormal joint position or reduced range of motion [2]. Gait abnormalities that result from trunk deviation can be seen as truncal sway in the sagittal and coronal planes. Abnormalities that stem from deviations at the hip include scissoring, circumduction, and Trendelenburg gait. Deviations at the knee include stiff knee gait, recurvatum, and flexed knee gait. Deviations at the ankle include equinous, dropfoot, high steppage gait and toe-toe gait. Gait deviations commonly occur in the pediatric population [2]. Gait analysis helps not only in evaluating abnormal walking patterns but it also directly impacts treatment planning. Clinicians and physicians can identify what surgical procedures are necessary in moving forward, what kind of prosthetics and orthoses can assist with abnormal walking patterns, physical therapies, and other varying forms of intervention. Gait analysis is conducted on healthy individuals as well in designing comparison studies or for "healthy/mean" data. Often times these data are used as control data.

Moissenet et al studied subjects with an instrumented knee prosthesis that allowed comparison of the estimated and measured medial and lateral knee contact forces during the gait cycle [11]. This study created a 3D lower limb musculoskeletal model based on a

one-step static optimization procedure which allowed simultaneous musculo-tendon, joint contact, and ligament and bone force estimation during gait. The purpose of this study in identifying musculo-tendon forces and joint reactions is different than most since musculo-tendon and joint reaction forces are typically estimated by first computing the musculo-tendon forces by static optimization and determining the joint reaction forces from the force equilibrium. *Moissenet et al* conducted a blind validation based on four sets of data assuming two conditions; one where only musculo-tendon forces were minimized and one where musculo-tendon, joint contact, ligament and bone forces were minimized. This study is an example of how motion analysis continues to advance in research and development. Subjects with gait deviations at the knee are undergoing this one-step optimization process in order to implement a quicker and more efficient way of calculating joint reaction forces. The model created in this experiment was able to estimate the timing of musculo-tendon forces during normal gait and was noted to be potentially able to estimate joint contact, ligament and bone forces and more specifically medial and lateral tibiofemoral contact forces during normal gait.

Subjects with neurological and musculoskeletal impairments can undergo gait rehabilitation with body weight unloading. The only issue with body weight unloading as a form of gait rehabilitation is that it is difficult to assess considering walking modality and the inability to maintain a comfortable speed when suspended by the body weight unloading system. *Fischer et al.* conducted a study where these two latter factors were constrained to a specific walking modality (overground as opposed to treadmill) and by devising a mechanical device that pulled the body weight unloading system at a constant speed. Although this study also recruited healthy subjects, the data is useful in assessing

future cases of patients with any neurological or musculoskeletal impairments with gait rehabilitation. Subjects were to walk overground under four experimental conditions. Initially they were to walk without a suspension vest (control) and then with 0% body weight unloading, 15% body weight unloading, and 30% body weight unloading. Spatiotemporal results showed that there were no statistically significant changes in cadence, speed, or stride length. There showed a reduction in double limb support and an increase in single limb support. Kinematic and kinetic results indicated significant reductions in lower joint kinematics and kinetics as body weight unloading conditions increased. Therefore it was concluded that overground gait with up to 30% body weight unloading reduced joint loads while walking at a constant speed.

Lanthrop-Lamback conducted a study on healthy individuals to determine the presence and prevalence of asymmetry in their lower extremity joint moments during overground walking [12]. Bilateral gait data were pooled from 182 healthy subjects. Four distinct populations were identified based on age, activity level, and body mass index. Mean peak external joint moments were determined from overground walking trials at a walking speed comfortable to each subject. For each subject right and left limbs were classified as "greater" or "lesser" moment to prevent obscuring of absolute asymmetry (averaging of positive and negative asymmetries across all subjects). In order to assess asymmetry *Lanthrop-Lamback et al.* used the calculated peak joint moments, created an initial chosen cutoff value of 10%, and estimated confidence intervals for the proportion of subjects with greater than 10% asymmetry between limbs, which were estimated based on the binomial distribution. It was concluded that over half of the overall population exceeded the cutoff value of 10% asymmetry in peak hip and knee flexion and adduction

moments. These conclusions may have a significant impact on gait evaluations, specifically clinical evaluations or research that uses asymmetry as an outcome.

In the research study titled *Applications of Gait Analysis in Pediatric Orthopaedics* [2], *Jing et al*. discussed patient populations that benefit the most from gait analysis, different gait abnormalities and a systematic approach to observational gait analysis. *Jing et al.* also looks at gait analysis in regard to quantitatively identifying gait deviations and assisting with clinical decision-making. Major components of testing protocol, patient management, and utilization of gait analysis in various stages of clinical evaluation and treatment planning are also discussed in this article. Two specific cases are looked at in this study.

The first case involved a healthy 12-year-old patient with bilateral in-toeing. In-toeing is a gait pathology that can stem from improper rotational alignment at the pelvis, femur, tibia, or foot. This patient underwent computerized gait analysis as opposed to observational gait analysis since this particular abnormality is difficult to assess simply from observation. It was determined that the patient had normal strength at all joints by manual muscle testing. When testing range of motion the patient exhibited asymmetrical femoral rotation and significant deviation from the normal value of 45 degrees. She was also found to have bilateral femoral rotation internal to normal with internal foot progression angles throughout the gait cycle. After these observations were made from computerized gait analysis, a surgical recommendation was made for bilateral femoral de-rotational osteotomies followed by physical therapy. One year after the surgical procedure the patient underwent postoperative gait analysis. The postoperative clinical examination concluded improved femoral rotation with foot progression angles within

normal ranges. These standardized outcome measures helped quantify functional changes and measure the patient's overall quality of life. The patient no longer has pain in her hips and is able to participate in physical activities with her peers without the incidence of tripping.

The second case this study looked at involved an 11-year-old patient that was diagnosed with left hemiplegic CP. She was experiencing a slower walking speed than her peers, decreased endurance, and frequently stumbled. The patient sought to improve decrease their pain and improve stability. As gait deficits are common with CP, computerized gait analysis was the best option to analyze problems the patient was having in the sagittal, coronal, and transverse planes. Key findings from gait analysis showed that she suffered from increased knee flexion with stiff-knee gait and also exhibited toe-toe gait pattern both on the left side. It was recommend after gait analysis that the patient underwent a left hamstring lengthening, rectus femoris transfer, and a tendo Achilles lengthening. In this study as well a year after the patient's surgery a postoperative gait analysis was performed. The surgery decreased knee flexion in gait, increased knee arc of motion, and ultimately achieved a plantigrade gait. The patient reported improved stability, decreased knee pain, and less frequent stumbling, all of which the patient hoped to correct with surgical intervention. Postoperative care is just as important as preoperative care. It not only evaluates the result of any type of intervention but it also provides insight to things that were not as apparent in previous studies.

Previous studies of gait within the population of patients suffering from chronic ankle instability have inconsistent findings. *Gigi et al.* [13] conducted an experiment to examine spatiotemporal gait parameters in CAI patients and determine the relationship

between self-reported disease severity and the magnitude of gait abnormalities. 44 CAI patients and 53 healthy control subjects were recruited for this experiment. Spatiotemporal gait analysis was conducted via a computerized mat and with the Short Form (SF) – 36 health survey. The results of this experiment showed that the CAI patients exhibited a 16% slower walking velocity, 9% lower cadence and approximately 7% lower step length. The base of support during walking was 43% wider for CAI patients. And the single limb support phase for CAI patients was 3.5% shorter compared to the control subjects. The 8-subscales of the SF-36, the physical component summary of the SF-36, and the mental component summary of the SF-36 were all significantly lower in the CAI patients compared to the control subjects. A significant correlation was also found between the mental and physical component summaries and most of the objective gait measures. Therefore it was concluded that there are significant differences in spatiotemporal parameters and that patients with CAI have a much wider base of support during walking. Overall these results highlight the usefulness of gait metrics and self-evaluation questionnaires in assessing the severity of disease in CAI patients.

F. Limitations of Motion Analysis

As useful and practical motion analysis is, there are a few limitations. Acquiring an entire motion analysis capture system is very costly. The price of an entire motion analysis capture system can range from $50,000 - $300,000. A breakdown of

renting/using a motion capture system is broken down below by Motion Capture NYC

[14].

Table 1: Average cost to rent motion capture system [14].

System Rental	$1500/day
Studio Space Rental	$1000/day
Data Solving	$10/character second
Data Retargeting	$10/character second
Technical Director	$500
Director	$500
Video Reference	$250
Basic 3D Models	$300
Actor	$250

The charge for a gait study can be as high as $2000 [15]. In addition to these costs, there

are maintenance contracts for hardware and software that range from $30-$50,000.

Sheldon R. Simon in his *Quantification of Human Motion: Gait Analysis - Benefits and*

Limitations to its Applications to Clinical Problems also identifies the cost of full-time

laboratory personnel to be $250,000. In order to balance expenses with revenue, at least

15 studies per week for 50 weeks at $500 per study would need to be conducted. That

calculates to $375,000.

Variability in gait measurements is another limitation of motion analysis. Variability,

inaccuracy, and lack of reproducibility due to technical factors, test subject factors, or

subjective clinical interpretation factors must be minimized for gait analysis to be

valuable [15]. Motion measurement and parameters are calculated using certain

assumptions and are not the real raw data measured. The degree of error resulting from seemingly small measurement errors can actually be quite significant. For example varying segment parameter values in determining the mass and moment of inertia values by up to +/- 40% of the baseline value significantly affects most of hip kinetic estimates, but by only less than 1% of body weight [16]. The determination of joint centers also can have a significant impact on the kinematic results produced by any motion capture system. A hip joint center position miscalculated above or below 30 mm can affect angles and moments at the hip and knee up to at least 25% [17]. Errors related to musculoskeletal variability still remain in bony contours and muscle attachments. These errors can be seen in complex joints such as the knee and ankle/subtalar/talar joints that are assumed to be rigid bodies. There is inherent cross-talk about these joints and a single axis through the range of motion of that joint cannot be identified. As a result a knee alignment device (KAD) is used to better locate the exact position of the knee joint center by defining three axes of rotation at the knee. KADs are used during the standing static trial preceding dynamic walking/running trials. In commencing the dynamic walking trials, the KAD is replaced with a marker at the base of where the KAD was originally placed, the lateral femoral epicondyle. To compensate for the inherent cross-talk at the foot, additional markers are added to the foot to accurately determine movement of and at the foot.

G. Significance of Current Study

The Orthopaedic and Rehabilitation Engineering Center (OREC) and its outreach clinics are currently utilizing a low-cost OptiTrack motion capture system to conduct motion analysis on patients with cognitive and physical disorders. This motion capture

system involves the use of software in order to compute kinematics and kinetics. AMASS and Visual3D are used in conjunction to identify the marker locations on each subject and track motion. Visual3D is a biomechanics analysis tool for measuring movement and force data as collected by almost any kind of 3D motion capture system [18]. This biomechanics tool is able to calculate kinematics and kinetics of a dynamic model. It also includes features for optimization, signal processing and filtering, inverse kinematics, complex biomechanical modeling, forces and force structures, and much more [18].

For the purpose of this study, OpenSim software was used to create a 3D musculoskeletal model. OpenSim software is a biomechanical tool used to analyze movement and force data. The software is free for use in commercial or non-commercial settings as long as the software is not redistributed. It also has a graphical user interface (GUI) that allows users to visualize models as well as generate and analyze specific simulations. The OpenSim application programming interface (API) is fully open source and licensed under the Apache 2.0 license [19], which allows users to extend the software and add additional code and functions through Matlab scripting. Each model in OpenSim can be configured to have up to six degrees of freedom (DOF) at each joint. The OpenSim gait2392 model has 3 degrees of freedom at the hip and 1 degree of freedom at the knee and 2 degrees of freedom at the ankle. However the second degree of freedom at the ankle joint in the coronal plane is locked, so the ankle is only observed in the sagittal plane (model is 3-1-1). This means that OpenSim will analyze the motion of the hip in the x, y, and z plane of a 3D Cartesian coordinate system and will analyze the motion of the knee and ankle in the coronal plane (x direction). The kinematic results obtained from OpenSim will then be compared to the kinematic results obtained from Visual3D to

provide a thorough comparison and validation of the OpenSim model. OpenSim has many more functions and analyses than our existing Visual3D software. It is open-source and freely available software, cutting costs of conducting motion analysis in OREC's clinics. Also, due to it being open source, OpenSim can be edited to execute programmable functions through MATLAB scripting/coding. OpenSim is similar to Visual3D in that they are both validated systems that can calculate inverse kinematics (joint angle measurements) at the hip, knee and ankle joints. Additionally, OpenSim has the capability to calculate muscle length changes during ambulation as well, whereas Visual3D cannot.

Understanding how joint and muscle mechanics change is critical in developing strategies and therapies to improve orthopedic intervention in patients with walking disorders. Human walking requires multi-joint coordination that can be disrupted by damage to bones or musculature. New breakthroughs in motion capture allow for analysis of joint angles through OpenSim's open source software. By utilizing OpenSim, a model can be created that determines lower extremity joint parameters. A model like this will be able to analyze and assess subjects with joint pathologies through a thorough assessment of their lower extremities using a motion capture system paired with OpenSim. This coupled with the low-cost OptiTrack motion capture system will be able to replace Visual3D and cut costs of conducting motion analysis and augment our existing system in that both kinematics and muscle length changes can be computed. Understanding how the muscle-tendon length changes with respect to ambulation can allow physicians and clinicians to identify key abnormalities within their lower extremities. These abnormal patterns can then be further investigated into for correctional and therapeutic purposes.

The purpose of this experiment was to validate the OpenSim 3D musculoskeletal gait2392 model and assess its ability to calculate muscle-length changes during normal gait. This was done by comparing the inverse kinematics output from the Visual3D conventional gait model to that from the OpenSim gait2392 model. The muscle-tendon length data obtained from this sample population was then compared to muscle-tendon control data obtained from Shriner's Hospital. It was hypothesized that the kinematic output between both systems would yield the same results since the same function is being applied to the same sets of data, only in different software. It was also hypothesized that there would be differences seen in the muscle-tendon data between the experimental and control data since the sets of data came from different sample populations.

METHODS

A. Equipment

18 OptiTrack cameras were used with AMASS software to acquire 3D marker data. The cameras operate at 120 frames per second (fps) during motion capture. The OptiTrack Flex 13 cameras have 1.3 MP resolution, expansive 56 degree field of view (FOV) and on-camera processing. Each camera is equipped with a stock lens of 5.5 mm with a horizontal FOV of 56 degrees and a vertical FOV of 46 degrees. The imager size of each camera is 6.144 mm x 4.9152 mm and has a pixel size of 4.8 um x 4.8 um.

B. Calibration

Prior to data collection, the motion capture system had to be calibrated in order to detect marker movement. The 18 OptiTrack cameras were placed on tripods surrounding the capture volume with 1-2 cameras on each tripod to ensure the entire capture volume

could be seen. Each camera is able to capture a 2D view of the markers placed on the subject's body. Each marker must be visible by at least two cameras in order to determine the marker's 3D coordinates. Therefore multiple cameras are needed to determine 3D location relative to the location of the cameras and markers in each cameras 2D view. The use of multiple cameras is also beneficial in the case that some markers are blocked during motion capture either by the subject's swinging arms. The L-Frame (depicted in Figure 4) is placed in the center of the capture volume and represents the origin ((0,0,0) of a Cartesian coordinate system). It is critical that the L-Frame be clearly visible in the view of every camera so that the origin of the capture volume is well defined relative to the capture volume. It also defines direction within the coordinate system based on how it is placed on the floor. An AMASS calibration wand is then used to register motion detection within each of the camera (pictured in Figure 4). It is a tensioned cable with six markers evenly spaced on it. It is waved around the motion capture volume such that motion can be registered by the swinging of the wand with the cameras registering motion at 120 frames per second.
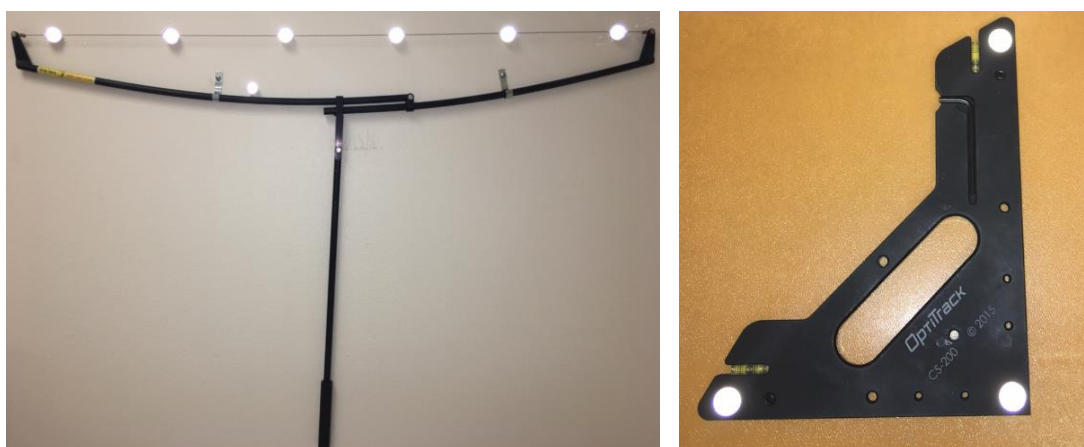
Figure 4: Calibration wand (left) and L-Frame (right) used for calibration.

C. Subject Population

A Power Analysis was conducted with pilot data processed in both Visual3D and OpenSim to determine a sample size. The Power Analysis conducted at 80% power at the 95% confidence interval yielded anywhere from 15-20 subjects as an adequate sample size to conduct this experiment for significant results. Therefore at least 20 subjects were required to complete this study. A limit of 30 subjects was specified in the scenario the data collected cannot be used further for analysis (e.g. marker dropout, testing error, or subject non-compliance). Due to the dropout rate in previously conducted studies, an additional 10 participants would be sufficient for analysis. A total of 24 subjects were recruited and the data from 20 of them were used. The reason that only 20 out of the 24 subject data were used was due to severe marker dropout seen in 4 of the 24 recruited subjects. 10 dynamic trials were taken for each subject upon scaling. The three best dynamic trials for each subject were analyzed. The subject population consisted of healthy individuals ranging between the ages of 18 and 35. A pre-screening questionnaire was handed to each potential subject to determine whether or not they were qualified for the experiment. The pre-screening questionnaire inquired about balance disorders, neurological problems interfering with walking, orthopedic issues, or any type of pain whilst walking. Table 2 depicts all the de-identified information collected from each of the 20 subjects.

Table 2: **Sample population measurements and information.**

Subject	Gender	Age	Height(m)	Weight(kg)	ASIS distance (in)	Left Leg Length (in)	Right Leg Length (in)	Left Knee Joint Diameter (cm)	Right Knee Joint Diameter (cm)	Left Ankle Diameter (cm)	Right Ankle Diameter (cm)
1	Female	26	1.732	64.1	9.8	35.25	34.875	10.8	10.9	6.0	6.3
2	Male	20	1.730	62.6	9.875	36.25	36.5	9.4	9.6	6.8	6.9
3	Male	20	1.773	80.8	10.0	36.75	36.375	10.5	10.75	7.8	7.6
4	Female	21	1.649	68.4	11.125	35.675	35.75	11.8	11.8	6.1	6.3
5	Male	20	1.772	93.4	10.5	37	36.625	11.1	11.3	7.1	7.3
6	Female	20	1.525	48.0	8.875	33.375	33.5	9.3	9.3	6.0	6.1
7	Male	22	1.771	61.1	9.75	37.625	37.75	9.6	9.5	6.6	6.9
8	Male	31	1.866	69.8	10.125	39.375	39.25	10.9	10.8	7.7	7.5
9	Female	30	1.613	71.7	10.125	33.675	33.875	11.5	11.5	6.9	7.1
10	Female	24	1.713	65.8	10.5	36.625	36.625	10.2	10.4	7.3	7.3
11	Female	21	1.704	59.8	10.0	35.25	35.0	10.3	10.4	6.7	6.5
12	Female	20	1.629	57.0	9.625	32.625	32.725	9.2	9.2	6.3	6.5
13	Female	21	1.903	86.23	11.105	39.255	39.295	10.6	10.5	7.5	7.5
14	Male	21	1.943	88.9	11.125	39.375	39.375	10.8	10.6	7.5	7.6
15	Female	30	1.753	74.1	10.48	36.68	36.8	10.5	10.3	6.6	6.8
16	Male	30	1.748	73.6	10.5	36.75	36.5	10.5	10.4	6.8	7.0
17	Female	26	1.681	61.2	10.78	36.65	36.55	9.8	9.8	6.5	6.4
18	Female	26	1.678	61.6	10.75	36.75	36.5	9.9	9.9	6.5	6.3
19	Male	32	1.879	85.7	9.4	40.25	40.5	10.7	10.9	7.5	7.5
20	Male	25	1.892	84.6	9.375	41.25	41.5	10.8	10.6	7.6	7.4

D. Marker Set

Although there are multiple marker sets that can be used in gait analysis, the marker set used for this study is known as the modified Helen-Hayes marker set. This marker set includes markers at the right anterior superior iliac spine (R_ASIS), left anterior superior iliac spine (L_ASIS), posterior superior iliac spine (PSIS), right and left hip (R_THIGH, L_THIGH), right and left lateral femoral epicondyle (R_KAX, L_KAX), right and left mid-shank (R_SHANK, L_SHANK), right and left lateral malleolus (R_ANKLE, L_ANKLE), right and left calcaneus (R_HEEL, L_HEEL), and right and left 2nd metatarsal head (R_META, L_META). Wand markers are typically placed mid-femur and mid-shank as shown in Figure 3. However since no wands were available during this study, an anterior thigh (R_ANT_THIGH, L_ANT_THIGH) and anterior shank marker were used (R_ANT_SHANK, L_ANT_SHANK). Replacing the wands with thigh and shank markers and anterior markers collinear to the thigh and shank markers provided additional tracking targets since no wands were available for use. The purpose of using wands on the thigh and shank segments in gait analysis is due to the extra adipose and muscle tissue on the thigh and shank. All the other markers are placed on bony prominences on the lower extremities where there is far less adipose or muscle tissue if any. Thigh and shank wands use a pair of markers to define the axial orientation of their respective segments. Wands provide a solution for registering bone-pose whilst permitting rapid attachment to non-anatomical position [20].

E. KAD System of Equations

During the static trial the KAD served the purpose of defining the frontal plane of the thigh segment. Upon beginning the dynamic trails, the KAD was replaced with a single marker on the femoral lateral epicondyle. This change of marker sets is accounted for in AMASS by inputting a dynamic marker file, which replaces the KAD with the knee marker. However in OpenSim once the static trial is loaded and scaled, the OSIM file does not account for the change in marker sets. Therefore a system of equations were created through Matlab to establish the position of the new dynamic knee marker during each dynamic trial.

This point is equidistant from the three KAD markers, such that the directions from the point to the three markers are mutually perpendicular. In order to pinpoint this exact location, a system of equations with three unknowns was established. Each location of the three KAD markers is a vector in a 3D Cartesian coordinate system. Using the distance formula and the measured length of the KAD markers to the center, the following equations were created:

$$d = \sqrt{(x_0 - x)^2 + (y_0 - y)^2 + (z_0 - z)^2}$$

$$d = 10\ cm = .1\ m$$

$$.01 = (x_1 - x)^2 + (y_1 - y)^2 + (z_1 - z)^2$$

$$.01 = (x_2 - x)^2 + (y_2 - y)^2 + (z_2 - z)^2$$

$$.01 = (x_3 - x)^2 + (y_3 - y)^2 + (z_3 - z)^2$$

Variables x, y and z represent the unknown location equidistant from the three KAD markers. X1, Y1, and Z1 represent the known location of one of the three KAD markers. X2, Y2, and Z2 represent the known location of another one of the three KAD markers. X3, Y3, and Z3 represent the known location of the last of the three KAD markers. Since square roots are involved in this system of equations, two sets of values are produced for x, y, and z.
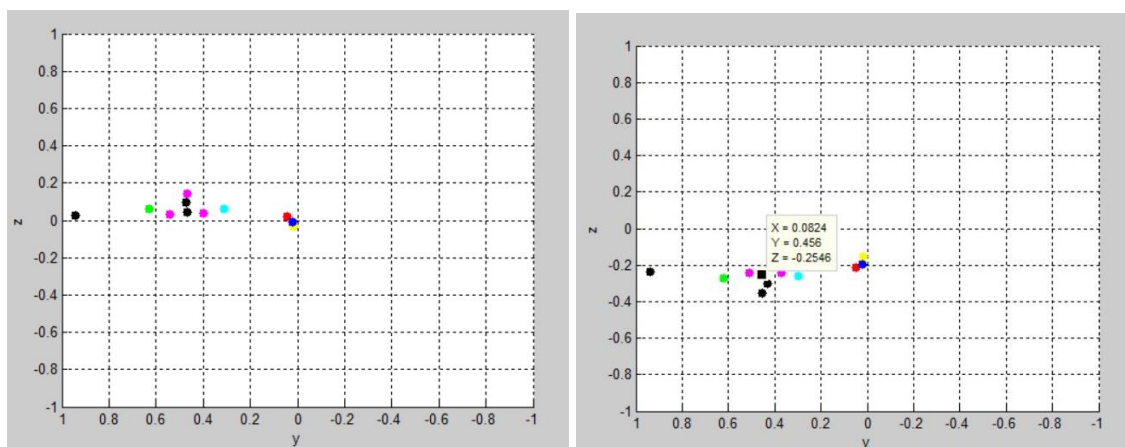
Figure 5: Coronal plane view of the markers on the right (left) and left (right) lower extremities.

The left plot in Figure 5 depicts the markers on the right lower extremities in the coronal plane viewed from the back of the subject. The two calculated knee marker points are seen in black surrounded by the KAD markers (magenta points). The correct calculated knee marker point should be in the same plane as the two KAD markers that are already in the same plane. Matlab code was able to detect the lower z value of the two calculated z values and assign it as the new calculated knee marker position for the right limb. The right plot in Figure 5 depicts the markers on the left lower extremities in the coronal plane viewed from the back of the subject again. In this plot however, the three black points represent the third KAD marker and the two calculated z values, with the two calculated z values being the two greater z values of the three points. In this case,

Matlab code was written to detect the greater z value of the two calculated z values and assign it as the new calculated knee marker position for the left limb. This is how the knee marker was calculated using the KAD for the dynamic motion trials of gait analysis in this experiment.

F. Biomechanical Model

A 3D musculoskeletal model was created in OpenSim software with 3 degrees of freedom (DOF) at the pelvis and hip joint, and 1 DOF at both the knee and ankle joints (gait2392, 3-1-1 model). The angles of rotation at each joint are either taken with respect to the global coordinate system or with the limb segment proximal to it. Euler angles help in assessing the motion of one segment with respect to another in the global coordinate system. In the case of the pelvic coordinate system, the angles of rotation are taken with respect to the trunk coordinate system which is set as the global coordinate system. Joint angles at the hip are calculated by the local coordinate system of the thigh relative to the local coordinate system of the pelvis. Joint angles at the knee are calculated by the local coordinate system of the shank relative to the local coordinate system of the hip. Joint angles at the ankle are calculated by the local coordinate system of the foot relative to the local coordinate system of the shank. Euler's theorem states that any two independent orthonormal coordinate frames can be related by a sequence of rotations about coordinate axes, where no two successive rotations may be about the same axis. Therefore a set of orthogonal embedded axes for dynamic and reference segments must be defined, X1, Y1, Z1. In this experiment the X1 axis is defined as the direction of the walkway. The Y1 axis is defined as orthogonal to the X1 axis pointing upwards. And the Z1 axis is orthogonal to both of these two axes. If an angle is rotated about the Z1 axis, the resulting

kinematics are defined in the sagittal plane as pelvic tilt, hip flexion and extension, knee

flexion and extension, and ankle dorsiflexion and plantarflexion. Once a particular

segment has rotated about a reference axis, the local coordinate system has a new

orientation, X2, Y2, Z2. If a segment rotates at an angle about the X2 axis, the resulting

kinematics are defined in the coronal plane as pelvic obliquity, hip abduction and

adduction, knee varus and valgus, and foot progression angle at the ankle. Now the local

coordinate system is reoriented once again, X3, Y3, Z3. If a particular segment has

rotated at an angle about the Y3 axis, the resulting kinematics is defined in the transverse

plane as internal and external rotations at the pelvis, hip, knee, and ankle. A breakdown

of the rotations can be seen in the matrix depicted in Figure 5.
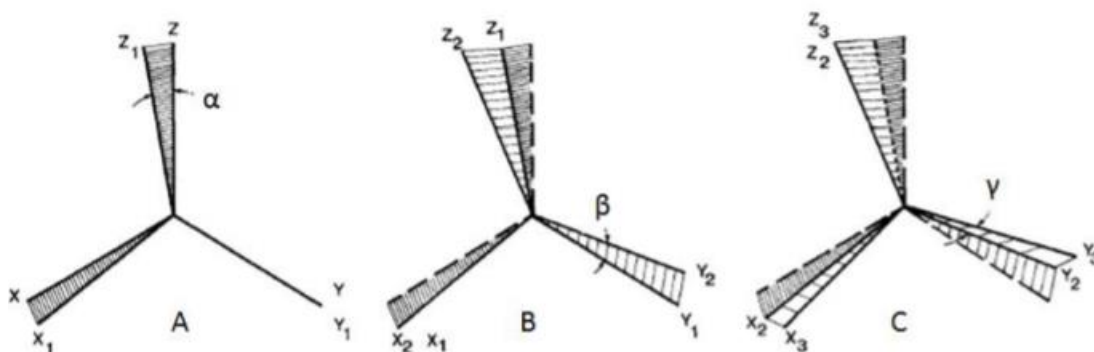
Figure 6: Euler Rotation [9].

Spatiotemporal parameters are also an important aspect of gait analysis.

Spatiotemporal parameters calculated during gait analysis can include walking speed,

stride width and length, cycle time, step length, steps per minute, strides per minute,

double limb support time, initial double limb support time and terminal double limb

support time. But for the purposes of this study only walking speed, stride length and

cadence were determined from each subject. Walking speed is defined as distance traveled per unit time. Cadence is the total number of steps taken in one minute. And stride length is defined as the distance between consecutive heel strikes of the same foot.

G. AMASS Software

AMASS software (ADTech Motion Analysis Software System) is a biomechanical assessment tool for pinpointing the 3D locations of each marker captured by the OptiTrack cameras and writing the data to file in C3D formatting. For the extent of my research AMASS was utilized to pinpoint the marker centroids in each camera's image coordinate system. A marker file with a list of the names of marker locations is input and tied in with each C3D file to establish the continuously moving position of each marker. Two types of marker files are used to establish the position of the markers. When the standing static trial is taken, a knee alignment device (KAD) is placed on the subject's knee in order to better establish the position of the knee joint center in 3D space since it is a complex joint. Therefore the static marker file is different than the dynamic marker file in that it takes into account the three markers on the KAD whereas the dynamic marker file simply has one marker at the lateral femoral epicondyle. Both the static and dynamic marker files used in this study mimic the modified Helen-Hayes marker set. The three KAD markers in the static marker file are labeled as R_KAX, R_KAD1, R_KAD2, L_KAX, L_KAD1, and L_KAD2.

H. Visual3D Software

These C3D files were then input into Visual3D for motion analysis. Anthropometric data including height, mass, ASIS distance, leg length, knee width and ankle width were

input and tied in with the 3D musculoskeletal model for scaling accuracy. Upon scaling the model, each event of an entire gait cycle was labeled; starting with heel strike of either the right or left foot, toe-off of the collateral foot, heel-strike of the collateral foot, toe-off of the original foot, heel-strike of the original foot, toe-off of the collateral foot and finally ending with the heel-strike of the collateral foot. This encapsulates an entire gait cycle for both the right and left foot.
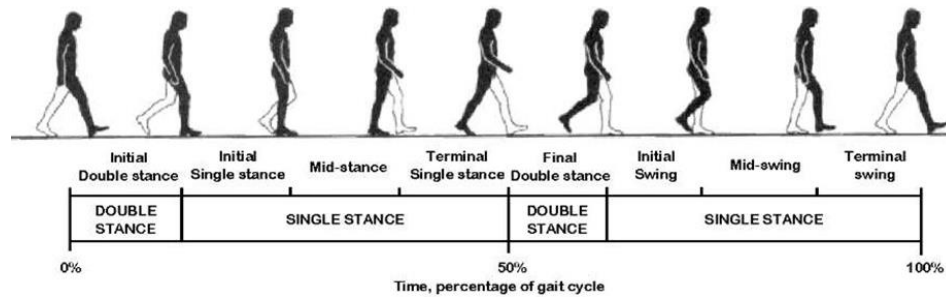
Figure 7: Steps of a full gait cycle [21].

The data is plotted against this calculated gait cycle length. Visual3D then plots and reports the kinematics of each dynamic trial. A data set of healthy individuals between the ages of 19 and 24 [9] was obtained to compare with the kinematic results obtained from the AMASS C3D files.

I. OpenSim Software

Barre et al. developed an open-source and multi-platform framework to read, write, modify and visualize data from any motion analysis systems using standard (C3D) and proprietary file formats [22]. *Mantoan et al.* also created a Matlab toolbox to process motion data for neuromusculoskeletal modeling and simulation [23]. SimTK is a free project-hosting platform for the biomedical computation community. This platform provides a Biomechanical Toolkit similar to those mentioned above, that processes C3D

data that is available for download. This toolkit serves as an interface between OpenSim and Matlab so that further scripting through Matlab and XML files can be done if necessary. This toolkit also provides Matlab-OpenSim pipeline tools to initiate the scaling process for biomechanical models along with initiating inverse kinematics calculations.

The toolkit also contained XML read/write functions that interfaced with OpenSim. One of the XML files wrote the basis of how subjects are scaled. In OpenSim, the body scale factor is computed by the distance between two markers. The pelvis is scaled by the distance between the left and right ASIS markers. The thigh is scaled by the distance between the ASIS and knee markers. The tibia is scaled by the distance between the knee and ankle markers. And the foot is scaled by the distance between the heel and metatarsal markers. Another XML files included in the toolkit weighted the importance of each marker and whether or not it would be used during the inverse kinematics solve. Each weight is given to a marker for solving inverse kinematics. The weight given to a marker is relative to the weight given to the other markers. The most accurately placed markers are typically weighted and turned on. These were the two XML files used in scaling each model. A set of XML files used in the inverse kinematics calculations were also included in the biomechanical toolkit. One of the XML files allowed users to turn on/off certain markers when solving for inverse kinematics and also weighted them. Again these markers were weighted based on accuracy of location.

When scaling each model, the model must be scaled from a control file into a new scaled model. This control OSIM file is known as the "gait2392" OpenSim (3-1-1 DOF-

IK) model and is a commonly used IK model [7]. As a 3-1-1 model, it Once the subject is scaled, this original model is overwritten and then used for inverse kinematics solve.

Along with the XML files, this biomechanical toolkit included starter-code for scaling models and calculating kinematics. These Matlab codes worked in conjunction with the read/write XML files to execute scaling and inverse kinematic calculations. However this code had to be edited in many ways to correctly scale and output results. Once the C3D files were obtained from AMASS, they were input into the Matlab scaling code to obtain a new scaled model. Upon scaling the model was ready for input into the Matlab inverse kinematics code to output plots of lower extremity joint angles. However in order to calculate inverse kinematics, coding for data characterization, data sorting, and filtering was written as part of data processing.

Matlab code was also utilized in calculating muscle length changes. For this part of the experiment, the OpenSim graphical user interface (GUI) was used. Once the inverse kinematics were determined, the variables used in that code were used in the Matlab code written to calculate muscle length changes. OpenSim has a function called Muscle Analysis, where a MOT file can be uploaded for the scaled subject's motion, and outputs an array of results including active fiber force, active fiber force along tendon, fiber active power, fiber force, fiber length, muscle-tendon length, fiber passive power, fiber velocity, moments and moment arms at each of the joints, muscle actuator power, normalized fiber length, normalized fiber velocity, passive fiber force, pennation angle, pennation angular velocity, tendon length, tendon force, and tendon power. For the scope of this experiment, the only output from this function needed was the muscle-tendon lengths. The Muscle Analysis function was used four times for each subject in OpenSim.

Once when loading the static MOT file to get original muscle-tendon lengths and again when loading the three best dynamic MOT files. Muscle-tendon length plots were plotted against a set of data collected by Adam Graf at Shriner's Hospital in Chicago, IL where he tested typically developing individuals whose age ranged from 6-18 years. The subject population had no history of neurological disorders, gait abnormalities, or orthopedic conditions.

II.   RESULTS

When determining the statistical significance of the results of this experiment, a paired t test was used for spatiotemporal parameter comparison and kinematic output comparison. A one sample t test was used for muscle-length variation comparison. Both of these statistical analyses were conducted at a 95% confidence interval.

A. Spatiotemporal Parameters

Table 3: Spatiotemporal parameters from Visual3D and OpenSim.

Visual3D					OpenSim			
Subject #	Stride Length (m)	R_cadence (steps/min)	L_cadence (steps/min)	Speed (m/s)	Subject #	Stride Length (m)	R_cadence (steps/min)	L_cadence (steps/min)	Speed (m/s)
50901	1.29	112.56	115.27	1.22	50901	1.29	115.54	112.52	1.22
51001	1.42	98.58	96.38	1.15	51001	1.43	97.82	96.65	1.16
62201	1.42	115.55	117.25	1.38	62201	1.42	119.99	114.38	1.40
62301	1.34	99.16	98.68	1.11	62301	1.36	99.64	96.65	1.12
62302	1.31	101.92	106.77	1.14	62302	1.33	100.11	98.07	1.11
63001	1.22	104.25	108.34	1.08	63001	1.22	107.48	105.33	1.08
70301	1.19	106.17	102.56	1.03	70301	1.19	103.80	105.19	1.04
70302	1.09	89.83	88.22	0.82	70302	1.09	88.04	90.03	0.81
70303	1.24	117.5	115.27	1.21	70303	1.24	116.19	115.62	1.25
70501	1.25	110.62	102.63	1.1	70501	1.25	105.83	103.99	1.10
70502	1.36	107.88	105.07	1.21	70502	1.36	104.33	102.87	1.20
70503	1.21	126.96	124.24	1.27	70503	1.22	124.84	125.56	1.26
70601	1.17	100.89	100.85	0.98	70601	1.17	99.68	101.09	0.98
70602	1.47	104.9	100.94	1.26	70602	1.47	104.90	103.39	1.26
70701	1.25	114.94	116.15	1.2	70701	1.25	115.50	113.86	1.20
70702	1.52	109.65	108.17	1.39	70702	1.53	112.12	106.97	1.37
71201	1.25	108.05	108.68	1.13	71201	1.26	104.36	108.67	1.13
71202	1.19	110.14	107.26	1.08	71202	1.19	111.39	107.39	1.08
71701	1.27	116.62	115.73	1.23	71701	1.06	117.42	117.53	1.24
71702	1.1	92.87	88.38	0.83	71702	1.10	91.45	87.91	0.83

Stride length, right-limb cadence, left-limb cadence, and walking speed were calculated spatiotemporal parameters in this experiment. When Visual3D calculates

spatiotemporal parameters, it averages the spatiotemporal parameters of each trial. Through scripting, Matlab was able to calculate the spatiotemporal parameters for each individual trial. Once they were calculated for the three trials per subject, they were averaged into one cumulative set of parameters per subject in order to compare to the values calculated in Visual3D. Table 3 displays the calculated stride lengths, cadences, and walking speeds for each subject. The differences between the parameters calculated in both software can be better viewed in Figures 8, 9, 10, and 11.
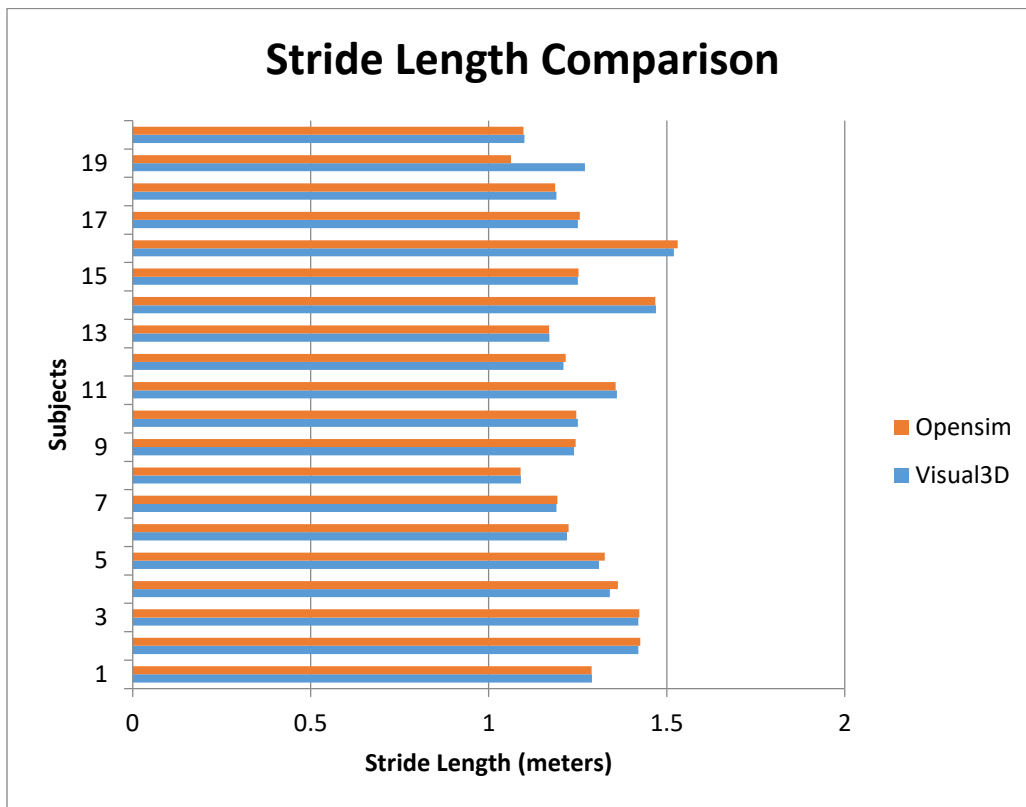
Figure 8: Stride lengths between OpenSim and Visual3D output.
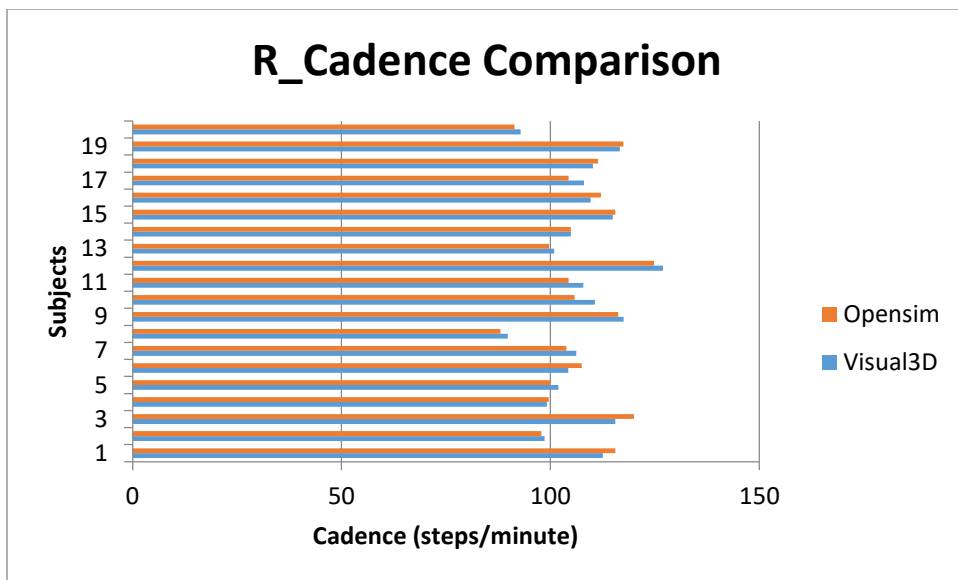
Figure 9: Right-limb cadence comparison between OpenSim and Visual3D output.
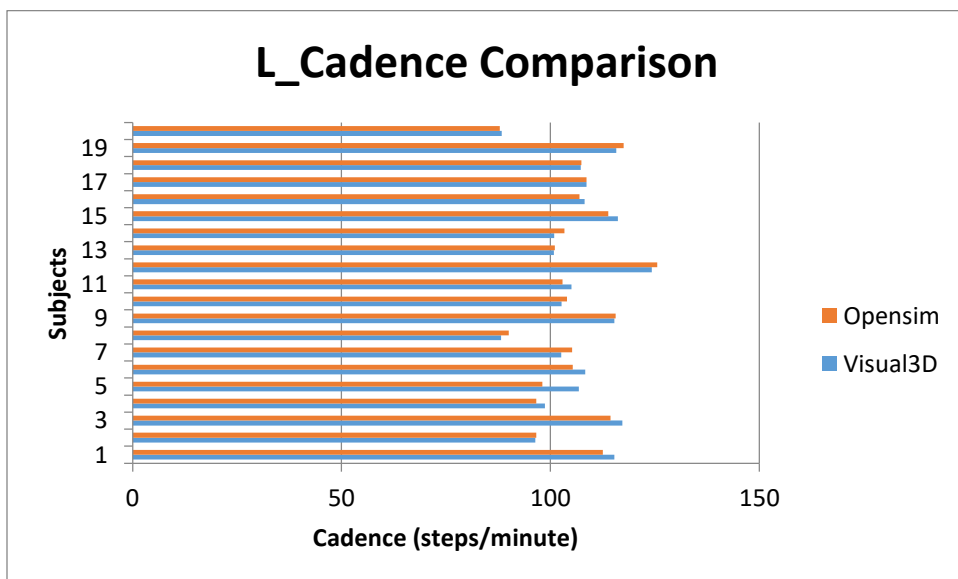
Figure 10: Left-limb cadence comparison between OpenSim and Visual3D output.
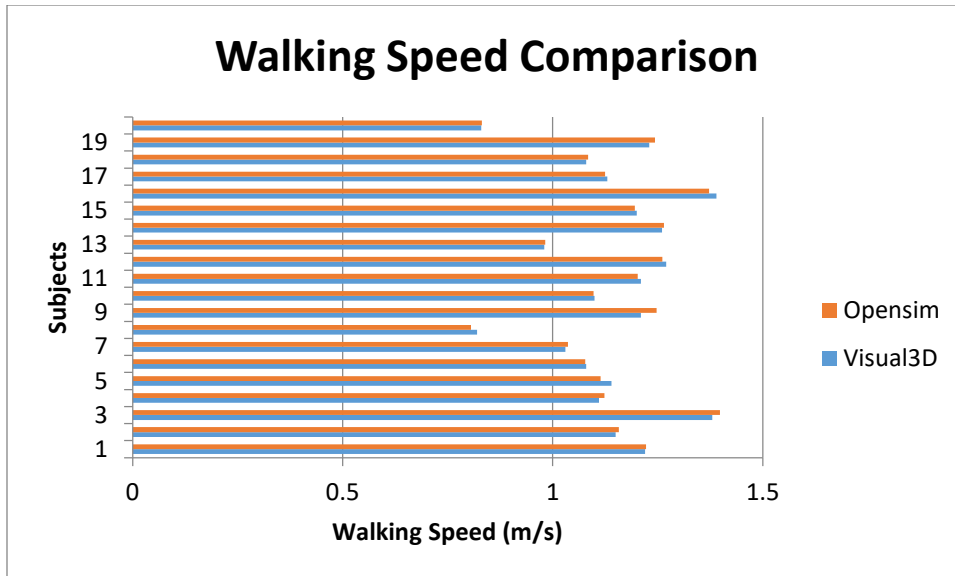
Figure 11: Walking speed comparison between OpenSim and Visual3D output.

B. Lower-Extremity Kinematic Analysis

Prior to collecting dynamic trial data the 3D musculoskeletal model must be scaled accordingly to each subject. Figure 12 represents a scaled 3D musculoskeletal model created in OpenSim. All the markers can be seen on this model based on the Modified Helen-Hayes marker set with the wands replaced by anterior thigh and shank markers. Figure 13 represents a scaled 3D musculoskeletal model created and validated in Visual3D. As seen, the model created and validated in Visual3D has thigh and shank wands incorporated into their marker model, which is exactly representative of the Modified Helen-Hayes marker set.
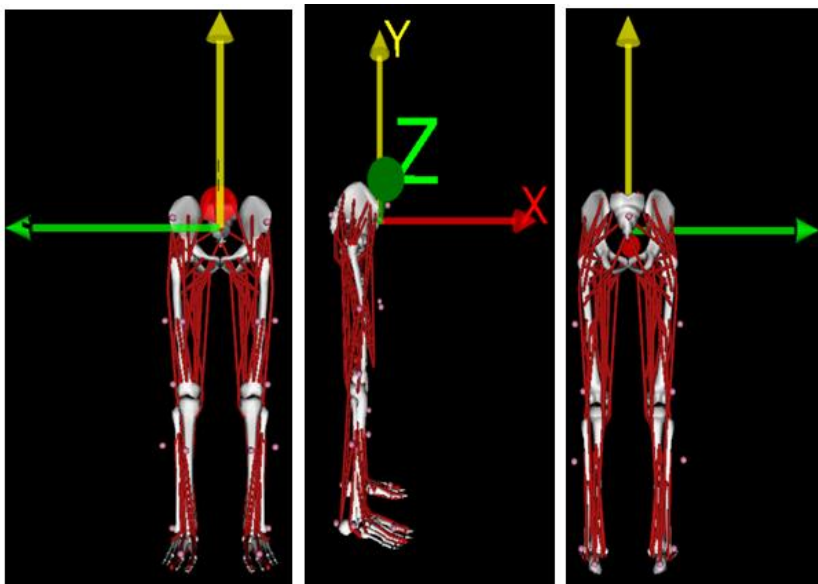
Figure 12: OpenSim 3D musculoskeletal model in sagittal and coronal planes.
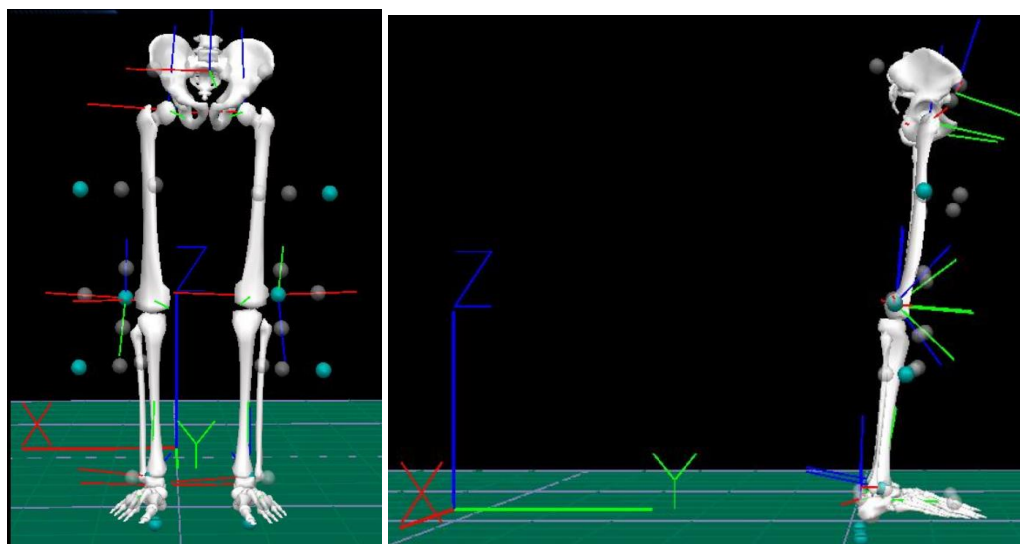
Figure 13: Visual3D musculoskeletal model in sagittal and coronal planes.

Figure 14 shows the kinematic joint angle data for all 20 subjects including each of their three best walking trials obtained from OpenSim. The three best dynamic trials were based on criteria including no marker dropout, normal ambulation at a comfortable walking speed and no tripping or tumbling. The kinematic output at the pelvis is shown in only one color since the pelvis is defined as one body in OpenSim, as opposed to Visual3D where to pelvis is defined as two separate bodies, respective to the motion at the right and left limbs.
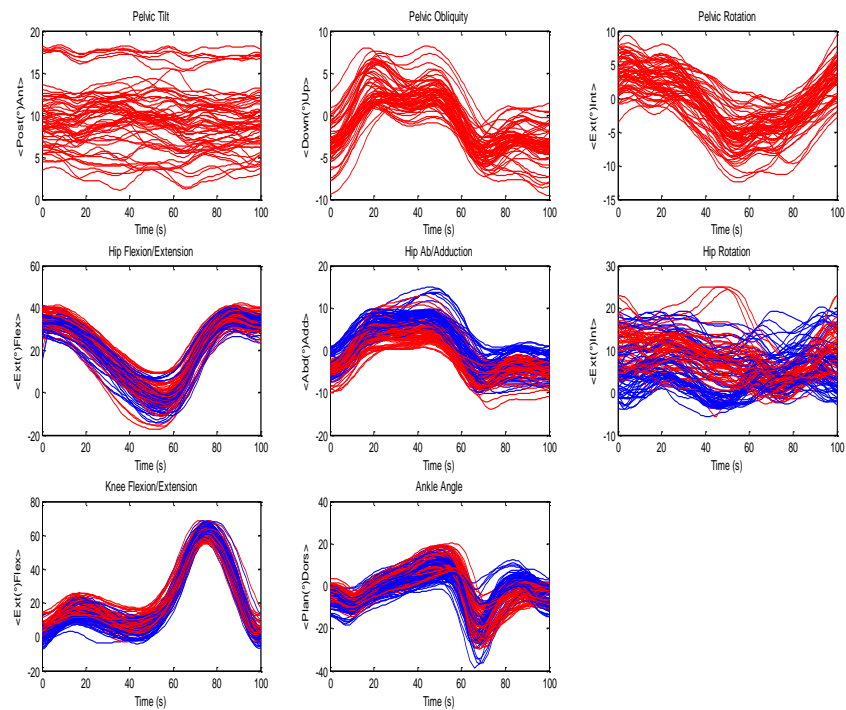
Figure 14: OpenSim left (blue) and right (red) limb kinematic output for 20 subjects' 3 best dynamic walking trials.

Figure 15 has been plotted the same way such that it displays the kinematic joint angle

data for all 20 subjects including each of their three best walking trials obtained from

Visual3D. The same three best dynamic trials were processed in OpenSim and Visual3D.
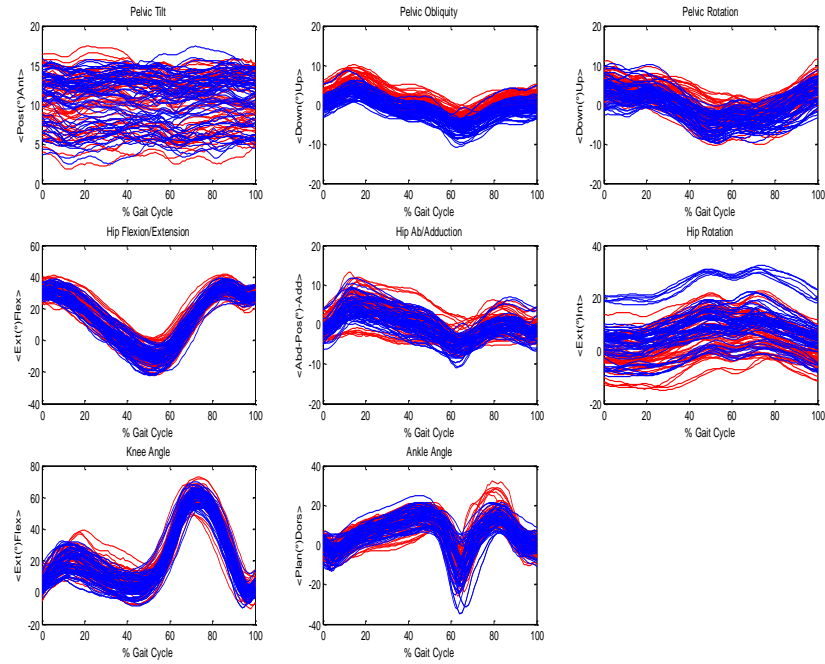
Figure 15: Visual3D left (blue) and right (red) limb kinematic output for 20 subjects' 3 best dynamic walking trials.

Figure 16 displays the kinematic output from Visual3D and OpenSim overplotted against each other with the OpenSim output in blue and Visual3D output in red.
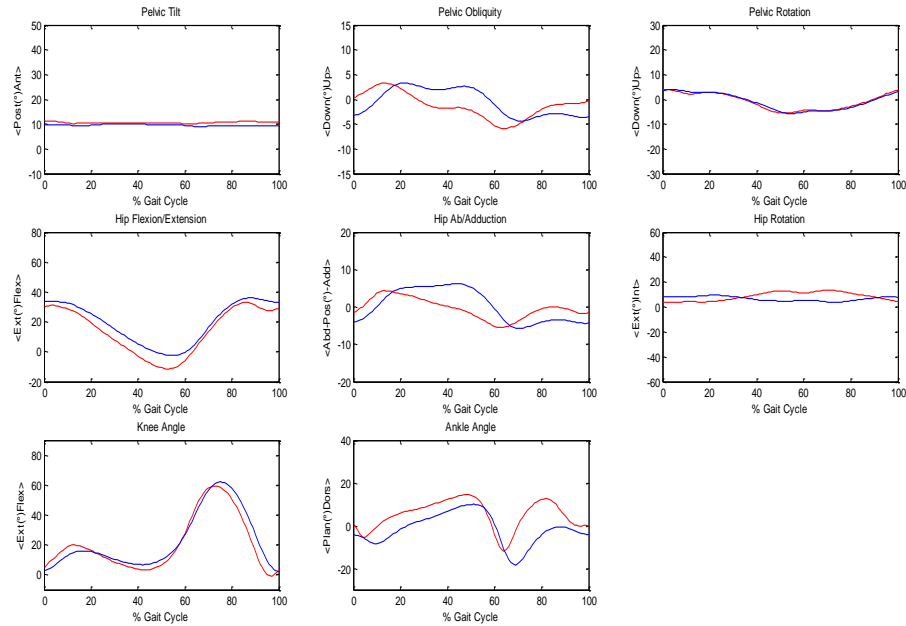
Figure 16: Kinematic output from OpenSim and Visual3D from same subject and same trial.

The plots in Figures 17 and 18 were consolidated by averaging the data and calculating the mean and standard deviation for all kinematic parameters. The mean and one standard deviation in both directions are plotted for the OpenSim and Visual3D outputs and displayed in Figures 17 and 18, respectively. The left limb and right limb data were combined prior to this for each joint.
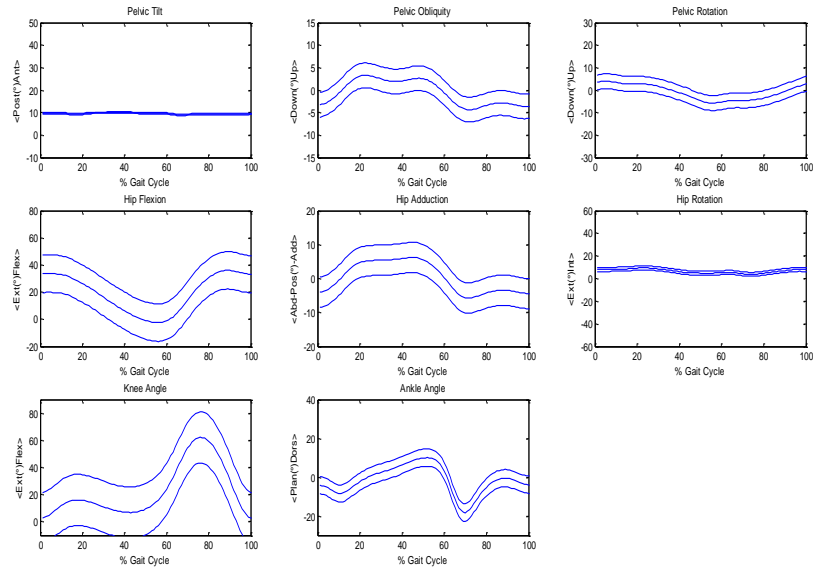
Figure 17: OpenSim mean and standard deviation kinematic plot of 60 dynamic trials.
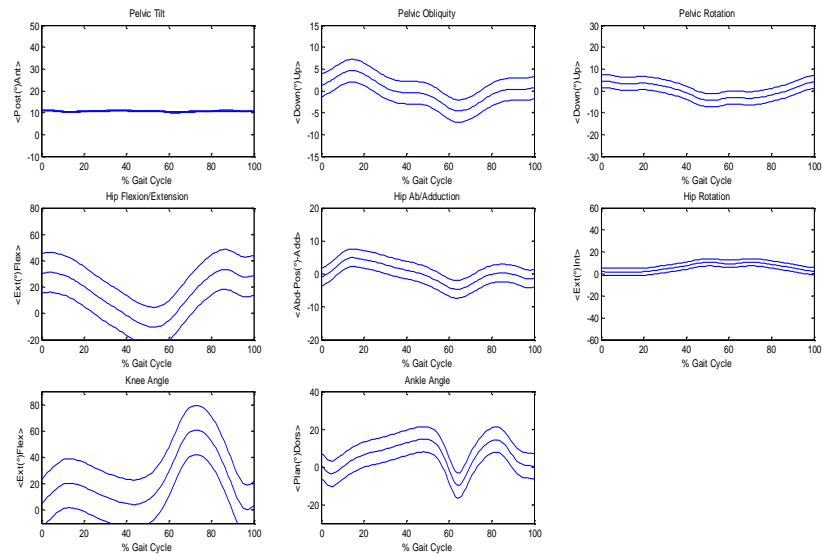
Figure 18: Visual3D mean and standard deviation kinematic plot of 60 dynamic trials.

C. OpenSim and Visual3D Comparison

The mean and one standard deviation in both directions from the OpenSim output and Visual3D output are over-plotted and displayed in Figure 19. This makes it easier to view the trends, similarities, and differences between the outputs from the different software during the same single gait cycle. The OpenSim output is displayed in blue and the Visual3D output is displayed in red. In order to really see the differences between the outputs, the difference was taken and plotted in Figure 20.
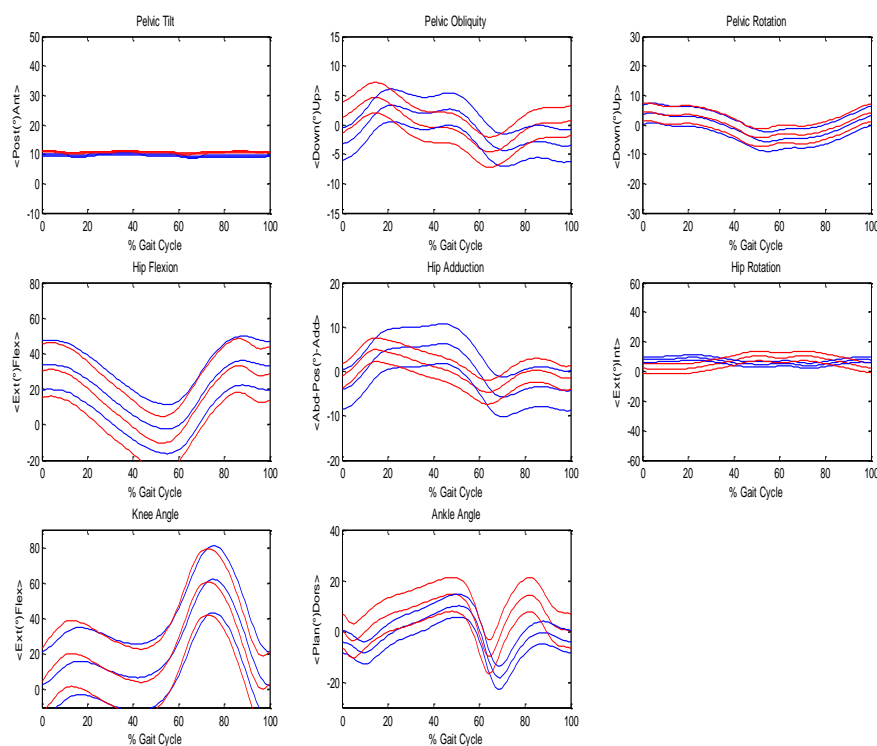
Figure 19: Mean and standard deviation kinematic overlap plot from OpenSim (blue) and Visual3D (red).
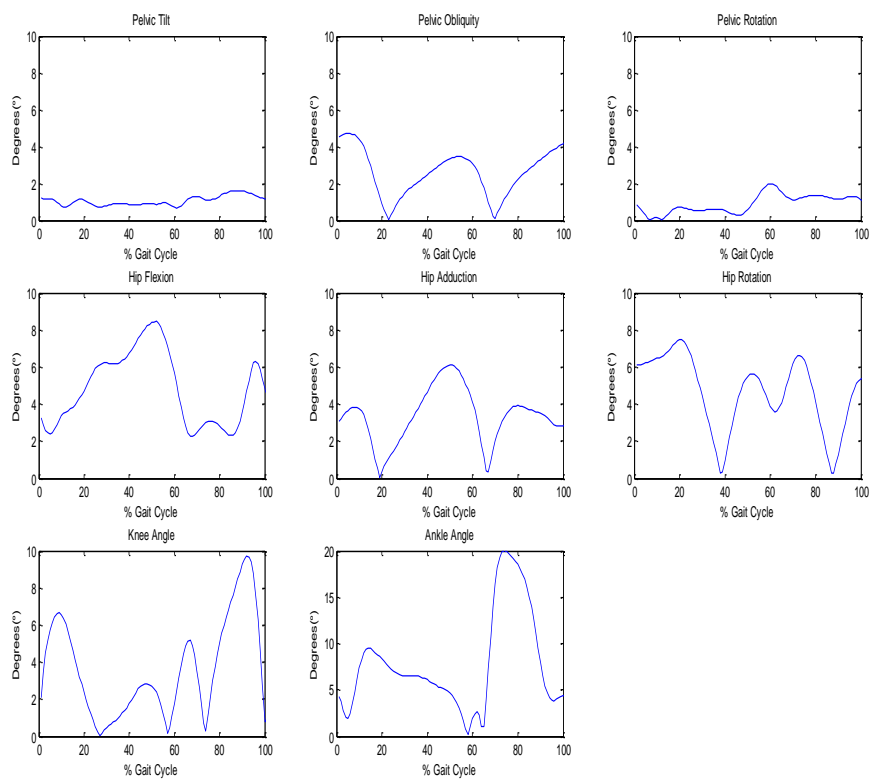
Figure 20: Absolute value of mean difference output plots between OpenSim and Visual3D.

D. Muscle-Length Variation

The second aim of this study was utilize OpenSim to calculate the change in muscle-lengths over the course of one gait cycle. OpenSim has an Analyze tool in their GUI that allows you to specify which type of analysis you want to conduct your scaled musculoskeletal model relative to a chosen dynamic walking trial. The shaded grey plots represent control data from healthy individuals between the ages of 6 and 18. They are plotted as normalized muscle-tendon length. This data is the quotient of dynamic muscle-tendon length (in mm) divided by the static muscle-tendon length (in mm). The blue plots overlaying them are the normalized muscle-tendon length outputs obtained from OpenSim. OpenSim's Analyze function can be specified further to a Muscle Analysis function, where specific muscles can be selected to determine different outputs of which include muscle-tendon length. To calculate the normalized muscle-tendon length, the dynamic muscle-tendon length output was divided by the static muscle-tendon length output. Therefore it is unit-less. The specific muscles in Figure 21 were chosen based on their overlapping presence in several published papers [24-28].
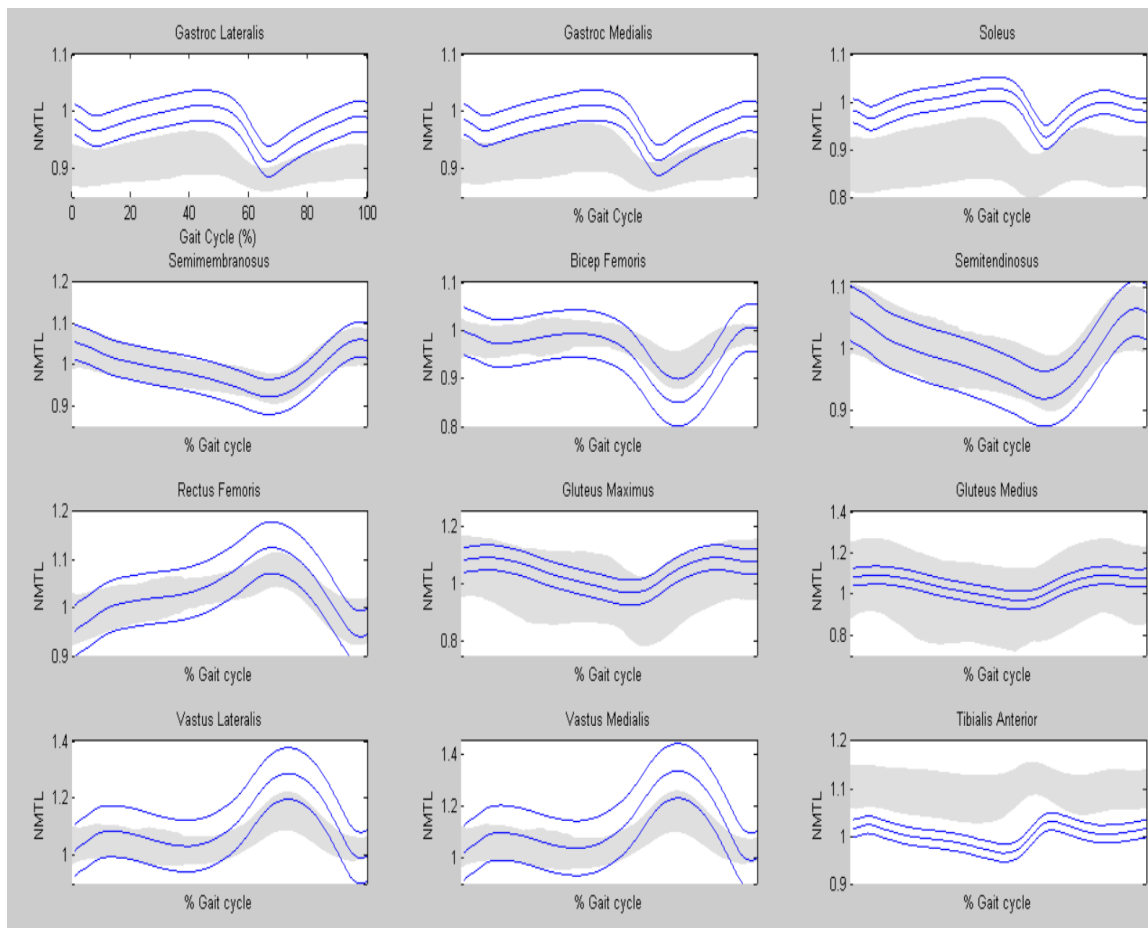
Figure 21: Muscle-length variation from experimental (blue) and control (grey) data during one gait cycle.

E. Statistical Analysis

The results being compared here are the kinematic output from OpenSim and the kinematic output from Visual3D; left limb output from OpenSim to left limb output from Visual3D and right limb output from OpenSim to right limb output from Visual3D. The kinematic parameters from both systems are also compared. Both kinematic outputs are obtained using the same sets of data but are calculated differently based on different scripting methods. A paired-T-test was conducted in Minitab at a 95% confidence interval in comparing these outputs. A paired t-test is used to compare two population means where you have two samples in which observations in one sample can be paired with observations in the other sample. There are three assumptions included when conducting a paired t-test. The dependent variable must be continuous. The dependent variable should be approximately normally distributed. And the dependent variable should not contain any outliers.

In this case the joint angles are the dependent variable and the independent variable is the length of the gait cycle. The joint angles in all planes of motion are continuous variables. In a paired t-test, the observations are defined as the differences between two sets of values. These observations are independent from each other. To determine whether or not the dependent variable was approximately normally distributed, z-scores were obtained from each set of joint angle data from both OpenSim and Visual3D and a correlation coefficient between the data and its corresponding z-scores was calculated. A good linear relationship is indicative of an approximately normally distribution of data. And finally it can be seen in the kinematic output plots from both OpenSim and Visual3D

that there are not outliers. Therefore these kinematic outputs were both eligible for paired

t-tests.

Table 4: Statistical analysis of right-limb kinematics.

Parameter		Mean (OpenSim) Stance Phase	Mean (Visual3D) Stance Phase	Difference in means	P-Value	Mean (OpenSim) Swing Phase	Mean (Visual3D) Swing Phase	Difference in means	P-Value
Hip Flexion/ Extension	Max Angle	32.155±4.757	32.11±4.131	.046±6.905	.959	33.622±4.393	33.722±4.105	-.099±6.536	.907
	Min Angle	-3.913±7.131	-9.912±6.466	6.00±10.89	<.05	-2.295±7.358	2.210±7.034	-4.51±11.69	.004
	Range	36.069±4.702	42.022±5.159	-5.953±7.66	<.05	35.918±4.636	31.511±5.408	4.406±7.294	<.05
Hip Ab/ Adduction	Max Angle	6.005±2.638	5.581±3.415	.423±.457	.457	-2.015±2.299	.876±2.545	-2.89±3.595	<.05
	Min Angle	-5.065±1.856	-4.173±2.194	-.893±3.05	.027	-8.868±2.26	-4.28±2.1	-4.59±3.412	<.05
	Range	11.070±2.733	9.754±3.293	1.316±4.545	.029	6.853±1.831	5.156±2.355	1.697±3.259	<.05
Hip Rotation	Max Angle	-.887±6.151	9.082±7.547	-9.97±11.39	<.05	-.781±2.593	8.639±6.697	-9.42±7.94	<.05
	Min Angle	-8.113±4.392	-1.547±6.057	-6.57±8.87	<.05	-7.483±4.037	.226±5.567	-7.71±8.01	<.05
	Range	7.266±3.00	10.630±3.014	-3.404±4.48	<.05	6.702±3.012	8.413±3.036	-1.71±4.161	.002
Knee Flexion/ Extension	Max Angle	25.699±4.221	43.13±7.048	-17.43±8.97	<.05	62.294±3.765	61.709±4.682	.585±6.07	.458
	Min Angle	2.746±4.353	2.972±4.702	-.227±6.295	.781	3.642±5.049	.435±4.712	3.207±7.037	.001
	Range	22.953±4.019	40.157±6.301	-17.2±8.15	<.05	58.652±5.991	61.273±5.274	-2.62±8.62	.022
Foot Dorsi/ Plantarflexion	Max Angle	12.244±4.264	15.371±-3.92	-3.127±6.11	<.05	5.433±4.875	16.241±5.441	-10.81±7.64	<.05
	Min Angle	-7.145±3.357	-9.734±5.356	2.589±5.866	.001	-18.128±7.39	-10.658±6.536	-7.47±8.76	<.05
	Range	19.389±2.618	25.105±5.070	-5.72±5.204	<.05	23.56±5.08	26.9±8.75	-3.34±9.62	.009

Table 5: Statistical analysis of left-limb kinematics.

Hip Flexion/ Extension	Max Angle	29.861±4.215	31.417±3.52	-1.55±5.128	.022	33.15±4.425	33.695±3.217	-.544±5.267	.427
	Min Angle	-6.447±5.792	-11.367±	4.92±8.22	<.05	-4.433±5.986	.38±7.185	-4.81±8.69	<.05
	Range	36.308±4.818	42.783±6.204	-6.48±8.69	<.05	37.584±4.168	33.315±6.461	4.268±6.624	<.05
Hip Ab/ Adduction	Max Angle	9.001±2.508	4.752±2.494	4.249±3.673	<.05	1.946±3.148	.264±2.007	1.682±4.024	.002
	Min Angle	-3.694±2.245	-5.537±1.976	1.843±3.193	<.05	-6.216±2.701	-5.615±1.975	-.601±3.545	.194
	Range	12.695±3.045	10.289±3.241	2.406±4.579	<.05	8.162±2.554	5.879±2.602	2.284±4.028	<.05
Hip Rotation	Max Angle	5.02±5.11	12.91±8.05	-7.89±10.97	<.05	1.68±4.5	13.37±8.03	-11.69±10.27	<.05
	Min Angle	-3.363±5.042	3.125±7.255	-6.49±10.34	<.05	-6.182±4.49	5.042±7.129	-11.22±8.73	<.05
	Range	8.38±2.765	9.786±2.727	-1.406±4.27	.013	7.864±3.094	8.333±2.684	-.469±4.633	<.05
Knee Flexion/ Extension	Max Angle	24.53±3.3	40.12±8.46	-15.59±9.1	<.05	63.947±2.754	60.694±4.33	3.253±5.017	<.05
	Min Angle	-.205±3.731	.822±4.371	-1.027±4.79	.102	.95±4.084	-1.243±3.757	2.194±5.242	.002
	Range	24.74±4.16	39.3±8.79	-14.56±9.42	<.05	62.997±4.995	61.937±5.032	1.06±7.26	.263
Foot Dorsi/ Plantarflexion	Max Angle	10.612±5.01	14.954±4.289	-4.34±6.835	<.05	4.102±4.528	13.695±3.906	-9.593±5.861	<.05
	Min Angle	-8.41±3.93	-11.62±8.36	3.21±9.2	.009	-18.69±8.25	-13.13±9.37	-5.56±11.63	<.05
	Range	19.019±2.84	26.569±7.235	-7.55±7.386	<.05	22.79±5.31	26.83±7.88	-4.04±8.57	.001

Table 6: Statistical analysis of pelvis as one body.

Parameter		Mean (OpenSim) Stance Phase	Mean (Visual3D) Stance Phase	Difference in means	P-Value	Mean (OpenSim) Swing Phase	Mean (Visual3D) Swing Phase	Difference in means	P-Value
Pelvic Tilt	Max Angle	8.508±4.202	11.812±-3.11	-3.304±5.57	<.05	7.81±4.275	11.392±3.093	-3.582±5.637	<.05
	Min Angle	6.03±4.414	9.337±3.335	-3.31±6.042	<.05	5.696±4.468	9.587±3.342	-3.892±6.139	<.05
	Range	2.479±6.527	2.475±.781	.003±6.309	.997	2.114±6.724	1.805±.566	.309±6.596	.718
Pelvic Obliquity	Max Angle	4.507±2.08	4.788±1.299	-.287±2.382	.355	-.56±1.576	.756±1.032	-1.316±1.926	<.05
	Min Angle	-3.801±2.118	-4.593±1.231	.793±2.807	.033	-5.652±1.679	-4.788±1.258	-.863±2.211	.004
	Range	8.301±2.401	9.381±2.464	-1.08±3.913	.037	5.092±2.059	5.545±1.738	-.453±2.808	.217
Pelvic Rotation	Max Angle	4.11±2.126	5.002±1.322	-.891±2.444	.006	2.244±2.732	3.822±1.928	-1.577±3.602	.001
	Min Angle	-5.88±2.832	-4.803±1.602	-1.08±3.198	.012	-5.961±2.61	-3.949±1.345	-2.013±3.219	<.05
	Range	9.991±3.302	9.806±2.804	.186±4.221	.735	8.206±3.5	7.771±2.593	.435±4.648	.471

Muscle-length data was collected from each subject and was compared to control data that was obtained and processed through OpenSim as well. The subject population from the experimental data obtained from this experiment were between the ages 18-35, had no balance disorders, no neuropathy or other neurological problems that interfered with walking, no orthopedic issues, and experienced no pain when walking. So although the subject population was different, muscle-length data was collected through OpenSim for both populations. Tables 4, 5, and 6 display the statistical results when comparing the mean of the experimental data to the mean of the control data. Since OpenSim defines the pelvis as one body and Visual3D defines the pelvis as two different bodies (left and right pelvis), the left and right pelvic data from Visual3D was combined and averaged in order to compare to the pelvis kinematics output from OpenSim.

A one sample T test was conducted in Minitab at a 95% confidence interval to compare the means of the data. When conducting a one sample t test, four assumptions must be made. The dependent variable must be continuous. Observations are independent from one another. The dependent variable should be approximately normally distributed. And the dependent variable should not contain any outliers. Both sets of data fulfill these assumptions. Both data sets were measured experimentally and are independent from one another due to the difference in sample populations. Figure 21 shows that there are no outliers in the data as well. Both mean data sets were normalized to the same amount of points and divided into stance and swing phase. The experimental data was separated by each subject's mean right and left toe-off from their three best dynamic trials. The control data on the other hand divided stance and swing phase at 60% of the gait cycle [29].

From there the maximum, minimum, and range of muscle-lengths were noted and compared between both data sets during stance and swing phase.

Table 7: Statistical analysis of muscle-length variation during stance phase.

	Muscles	Limb	P-Value		
			Maximum	Minimum	Range
Stance Phase	Gastroc Lateralis	Right	0	0	0
		Left	0	0	0
	Gastroc Medialis	Right	0	0	0
		Left	0	0	0
	Soleus	Right	0	0	0
		Left	0	0	0
	Semimembranosus	Right	0.004	0	0
		Left	0	0	0
	Bicep Femoris	Right	0.059	0	0
		Left	0.042	0	0
	Semitendinosus	Right	0.054	0	0
		Left	0	0	0
	Rectus Femoris	Right	0	0	0
		Left	0	0	0
	Gluteus Maximus	Right	0	0	0.002
		Left	0	0	0.002
	Gluteus Medius	Right	0.914	0	0
		Left	0.002	0	0
	Vastus Lateralis	Right	0	0.727	0
		Left	0	0.277	0
	Vastus Medialis	Right	0	0.66	0
		Left	0	0.382	0
	Tibialis Anterior	Right	0	0	0
		Left	0	0	0

Table 8: Statistical analysis of muscle-length variation during swing phase.

	Muscles	Limb	P-Value		
			Maximum	Minimum	Range
Swing Phase	Gastroc Lateralis	Right	0	0	0
		Left	0	0	0
	Gastroc Medialis	Right	0	0	0
		Left	0	0	0
	Soleus	Right	0	0	0
		Left	0	0	0
	Semimembranosus	Right	0	0	0
		Left	0	0	0
	Bicep Femoris	Right	0	0	0
		Left	0.001	0	0
	Semitendinosus	Right	0	0	0
		Left	0.003	0	0
	Rectus Femoris	Right	0	0	0
		Left	0	0	0
	Gluteus Maximus	Right	0	0	0.001
		Left	0	0	0
	Gluteus Medius	Right	0.338	0	0.001
		Left	0.175	0	0
	Vastus Lateralis	Right	0	0.001	0
		Left	0	0.007	0
	Vastus Medialis	Right	0	0	0
		Left	0	0.008	0
	Tibialis Anterior	Right	0	0	0
		Left	0	0	0

III. DISCUSSION

A. Spatiotemporal Parameters

The spatiotemporal parameters from OpenSim and Visual3D were averaged for all 20 subjects and summarized in Table 9. It can be seen that the difference in means from both systems are below 1.0 for all spatiotemporal parameters. The associated P-values are also displayed in Table 9. The statistical comparison conducted in comparing the difference in means was the paired t-test. These sets of data fulfilled all assumptions of a paired t –test. In this statistical analysis the null hypothesis is that the mean difference between paired observations is zero. With a 5% confidence interval, the p-values for all spatiotemporal parameters conclude that the null hypothesis is accepted and the results are statistically significant.

Table 9: Statistical analysis of spatiotemporal parameters.

Parameter	Mean (OpenSim)	Mean (Visual3D)	Difference	P-Value
Stride Length (m)	1.278	1.2709	0.0071	0.513
R_Cadence (steps/minute)	107.45	107.02	0.431	0.444
L_Cadence (steps/minute)	106.34	105.68	0.658	0.276
Walking Speed (m/s)	1.141	1.1421	-0.00112	0.72

B. Kinematic Analysis

The maximum, minimum, and range between the maximum and minimum joint angles were all calculated for the duration of stance phase and swing phase for all three trials of all 20 subjects. These values are displayed in Tables 4, 5, and 6. The difference in means in both stance and swing phase for the maximum and minimum angles in

comparing pelvic tilt were statistically different with p-values of 0. The difference in means in both stance and swing phase for the joint angle range of pelvic tilt was found to be .003 and .309 degrees, respectively. These results yielded p-values of .997 for the difference range in stance phase and .718 for the joint angle range in swing phase. Overall in both systems it can be seen from Figure 19 that the pelvis experienced slight anterior pelvic tilt which is what is expected (Figure 28). Normal values of anterior pelvic tilt seem to range between 6-13 degrees [30]. The differences between the outputs from both systems are minimal as seen in Figure 20.

When comparing pelvic obliquity, conducting a paired t-test to determine whether the difference in means yielded the same results as for pelvic tilt when comparing the minimum joint angle with p-values of .033 and .004 in stance and swing phase, respectively. The difference in means for the maximum angle in stance phase yielded a p-value of .355 and 0 in swing phase. The p-value for the range of pelvic obliquity in stance phase was calculated to be .037 but .217 in swing phase. As seen in Figure 19 the Visual3D output began with more upward obliquity than OpenSim output at the beginning of the gait cycle. However the OpenSim output suggests more upward obliquity during the middle through end of stance phase and consistent downward obliquity following toe-off. Visual3D pelvic obliquity shows more upward obliquity following toe-off.

Finally looking at pelvic rotation, the p-values for maximum and minimum pelvic rotation angles in both stance and swing phase were less than .05 and were concluded to be statistically different. But the p-values in stance and swing phase for the range of

pelvic rotation were .735 and .471. The differences between the outputs from both systems are minimal as seen in Figure 20.

The pelvis is defined as two separate bodies outlined by three different points in Visual3D. The right pelvis is defined by the RASIS marker, PSIS marker, and the right hip joint center. The left pelvis is defined by the LASIS marker, PSIS marker, and the left hip joint center. OpenSim on the other hand defines the pelvis as one body, defined by the RASIS, LASIS, and PSIS markers. The data from the left and right pelvis from Visual3D were averaged in order to conduct a statistical comparison between the pelvis in Visual3D and OpenSim. The difference in how the pelvis is defined in each system may be attributed to the differences in the kinematic output in all three planes of the pelvis.

The hip, knee, and ankle joints were analyzed separately from right and left limbs. Comparing range and minimum right and left hip flexion/extension angles, the difference in means yielded p-values less than .05 in both stance and swing phases. The maximum right hip flexion/extension angle yielded p-values of .959 and .907 in stance and swing phase, respectively. The left maximum hip flexion/extension angle resulted in a p-value of .022 in stance phase and .427 in swing phase. But since the paired t-test was carried out with a 5% confidence interval the left maximum hip flexion/extension angles in stance phase from OpenSim and Visual3D are deemed statistically different. Although the hip flexion/extension plots from both systems started at the same point of hip flexion, the Visual3D output experienced lesser hip flexion than the OpenSim output throughout all of stance phase. During swing phase the difference between the plots were smaller

with the OpenSim output experiencing slightly higher hip flexion at the end of the gait cycle.

All the p-values for comparing hip abduction/adduction in stance and swing phase for the maximum, minimum and range were less than .05 except for the max hip ab/adduction angle during stance phase which yielded a p-value of .457. The OpenSim output shows that the hip experienced longer hip adduction throughout stance phase as opposed to the Visual3D output showing the hip abducting until toe-off after the initial adduction at the beginning of the gait cycle. During swing phase both system outputs showed slight hip adduction.

All the p-values for comparing hip rotation in stance and swing phase for the maximum, minimum and range were less than .05, concluding that the hip rotation joint angles were statistically different between both systems. The two system outputs display in Figure 19 that the hip was internally and externally rotating at different times. The system outputs did not follow the same pattern. However the differences between the plots remained below 10 degrees throughout the entire gait cycle. The reason that the hip kinematics differ so greatly in the coronal and transverse planes is due to the fact that an anterior marker was used on the thigh and shank as opposed to wands. The musculoskeletal model in Visual3D assumes the use of wands and calculates kinematics based on their use and location. Therefore since the thigh is defined by different marker locations in each system, the results were not consistent.

Kinematics at the knee produced varying results. Comparing the right and left maximum knee flexion/extension angles in stance phase produced a p-value of 0.

Comparing the right maximum knee flexion/extension angle in swing phase however produced a p-value of .458.The maximum knee flexion/extension angles produced by the left knee resulted in a p-value of 0. The minimum right knee flexion/extension angles produced a p-value of .781 in stance phase and a p-value of .001 in swing phase. The minimum left knee flexion/extension angles produced a p-value of .102 in stance phase and a p-value of .002 in swing phase. Comparing the range of right and left knee flexion/extension angles yielded p-values of 0 in stance phase. In swing phase the right knee flexion/extension ranges resulted in a p-value of .022 and .263 for the left knee flexion/extension ranges. As seen in Figure 19, the kinematic output from both systems follow the same pattern. The output from Visual3D is seen to have higher knee flexion in the beginning of stance phase but the output from OpenSim is slightly more flexed during swing phase.

The kinematic output at the ankle joint from both systems follow a similar pattern however the statistical analysis shows that the difference in means are statistically different at the maximum and minimum foot angle as well as the range of the foot angle. The maximum dorsiflexion/plantarflexion angles for the right and left limbs yielded p-values of 0 in both stance and swing phase. The minimum dorsiflexion/plantarflexion angles for the right and left limbs yielded a p-value of 0 in swing phase. However in stance phase the right and left limbs yielded a p-value of .001 and .009 respectively for the minimum dorsiflexion/plantarflexion angles. When looking at the range of dorsiflexion/plantarflexion angles, p-values of 0 were seen at stance phase for both the right and left limbs. During swing phase p-values of .009 and .001 were seen for the right and left limb, respectively. Figure 19 suggests that when processed through Visual3D, the

foot experiences higher dorsiflexion throughout the entire gait cycle. The OpenSim plot suggests that the foot experienced more plantarflexion prior to toe-off and followed with far less dorsiflexion.

These variations in kinematic output between the two systems are reflective with the findings by Kainz et al [31]. Kainz et al. found that the method of determining kinematics, whether it be direct or inverse, does not have as great of an effect as when different anatomical models are used between the systems. The anatomical segment frames must be defined the same way in both models to get similar results. As mentioned earlier anatomical modeling entails anatomical segment frames as well as joint constraints. It was found that hip rotation between the Plug-in-Gait model and OpenSim model exhibited a root mean square difference (RMSD) of 11 ± 6 °, which was reduced by 55% when the OpenSim and Plug-in-Gait models were tested again with the same anatomical segment frames. This article demonstrates the importance of reliability of kinematic results with anatomical modeling. Since the biomechanical model used in OpenSim, gait2392, had different joint constraints than the biomechanical model used in Visual3D, the kinematic results varied.

C. <u>Muscle-Length Variation Analysis</u>

Tables 7 and 8 depict the statistical analysis of comparing the experimental data obtained in this experiment to the control data obtained from Shriners Hospital. A more in-depth statistical analysis can be seen in Appendix C where the mean values that were being compared are depicted. Table 7 shows that the only muscles during stance phase that showed no statistical differences were the bicep femoris, semitendinosus, gluteus

medius, vastus lateralis, and vastus medialis. The right bicep femoris had a P-value of .059 when comparing maximum mean values. The rest of the P-values obtained from the bicep femoris comparison were below .05 and were concluded to be statistically different than the control data. The P-value for right gluteus medius maximum mean value comparison in stance phase resulted in .914, concluding no difference. The vastus lateralis concluded similarities in minimum mean values for the right and left limb during stance phase with P-values of .727 and .277, respectively. When comparing the minimum mean values of the data in stance phase, P-values of .66 and .382 were calculated for the right and left vastus medialis, respectively and thus concluded statistical similarity between the data. The rest of the p-values for all the muscles analyzed in this experiment during stance phase for both the right and left limbs were below .05 and concluded that the maximum, minimum, and range values of muscle-lengths between the mean data sets were statistically different. During swing phase, the only muscle that showed statistical similarity between the two sets of data was the gluteus medius when comparing maximum mean values. P-values of .338 and .175 were calculated for the right and left limb, respectively. The rest of the p-values for all the muscles analyzed in this experiment during swing phase for both the right and left limbs were below .05 and concluded that the maximum, minimum, and range values of muscle-lengths between the mean data sets were statistically different.

As mentioned previously, the sample populations being compared were from different age groups. The control data was obtained from individuals ranging from 6-18 years of age and the experimental data obtained in this experiment were from individuals ranging from 18-35 years of age. The differences in mean output can definitely be

attributed to this fact. This control data was used to compare muscle-length change data during a single gait cycle only, not to validate OpenSim's validity in being able to calculate muscle-length changes during ambulation. OpenSim's ability to determine muscle length changes during an entire dynamic walking trial can be output through their graphical user interface as well and outputs the data in any specified location on the user's computer. Matlab scripting helped determine muscle-length changes during a specific gait cycle. The forces generated by muscles are highly dependent on their fiber lengths, yet it is difficult to measure the lengths over which muscle fibers operating during movement [24]. Changes in muscle-lengths during gait can be predicted by analyzing joint angle kinematics. Concentric and eccentric contractions during a gait cycle can be identified in flexion and extension in the sagittal plane, abduction and adduction in the coronal plane, and internal and external rotation in the transverse plane. Through these eccentric and concentric contractions, predictions can be made on the magnitude of muscle-length changes during a gait cycle. OpenSim's ability to calculate muscle-length changes makes it distinct from Visual3D. Although Visual3D also has numerous features in biomechanical analysis, muscle-length changes during ambulation is a key indicator in highlighting abnormalities in gait and can be extremely beneficial in studying motion analysis. With access to OpenSim's open-source software for developing and analyzing muscle-driven simulations, clinicians and researchers are able to establish quantitative, cause-effect relationships between muscle properties and movement in the laboratory [32].

D. Limitations / Causes of Error

Since the data set being input into both systems is the same, the output should theoretically be the same if not quite similar. One difference between the two systems in calculating inverse kinematics is the pose estimation algorithms they use. OpenSim uses a least squares approach to compute kinematics to minimize the difference between experimental marker locations and virtual markers on the model while maintaining joint constraints [33]. Visual3D on the other hand uses Segment Optimization or Global Optimization [9]. These methods work to create joint angle output where marker dropout was prevalent. Marker dropout could have been due to blocking of the cameras by desks or objects around the motion analysis lab or simply due to the inability of the camera to capture marker location due to hand swinging during ambulation. Pose estimation fills in those gaps by estimating the position of marker movement. Therefore due to this difference in pose estimation, the maximum, minimum and range of the joint angles could very well be slightly different from system to system.

Differences seen in the kinematic output from Visual3D and OpenSim may be due to different anatomical models used. Different anatomical models entail different anatomical segment frames and different joint constraints [31]. The gait2392 model has two degrees of freedom at the ankle, but the degree of freedom in the coronal plane is constrained in OpenSim. Since the ankle is such a complex joint and the foot has so many bones, constraining the motion in the coronal plane directly affects the kinematic output in the sagittal plane. This knee is also a very complex joint, and limiting it to one degree of freedom in the sagittal plane affects the kinematic output at the knee. The commonly

used model in 3D gait analysis, the conventional gait model, outputs three rotations at the knee, and thus the gait2392 model wouldn't be suitable in many clinical settings [7].

The difference in pelvic tilt angles can be attributed to the OpenSim model neutral position coinciding with the anatomical position as opposed to the neutral pelvic tilt in the Visual3D model which is defined by the anterior and posterior iliac spine markers [31]. This offset affects the lower extremity kinematics beyond the pelvis, especially the hip joint in all three planes of motion. This further asserts the claim of using consistent anatomical models across biomechanical systems in order to see similar results.

The kinematic output in the coronal and transverse planes is skewed due to the use of anterior thigh and shank markers rather than using wand markers. Although the anterior markers at the thigh and shank served their purpose to establish collinearity and help better define motion at the thigh and shank, they lack the rotational motion which is much better captured when using wand markers. But as seen in Figure19, the difference between the mean outputs from each system was consistently below 10 degrees in the coronal and transverse planes even though there was some fluctuation in difference. The hip ab/adduction plot in Figure 19 shows that both system outputs follow the same general trend. However the output from OpenSim shows a rise and consistency in adduction throughout stance phase. The Visual3D output on the other hand shows slight adduction in the beginning of stance phase followed by a steady decrease/abduction until swing phase. During swing phase the hip ab/adduction output from both systems follow the same trend. Figure 19 shows that the OpenSim output of hip rotation starts out at slight internal rotation at the beginning of stance phase and at mid stance phase begins to rotate externally until the swing phase where the hip begins to rotate internally again. The

Visual3D output depicts the hip starting at a neutral position and internally rotates throughout the remainder of stance phase and begins to slightly rotate externally during swing phase.

Another difference between the how the two systems calculate their respective kinematic outputs is the way that heel-strike and toe-off are defined. Both OpenSim and Visual3D allow users to induce step by step motion of the scaled OSIM model relative to the input dynamic C3D file. Visual3D allows users to see the frame-by-frame progression throughout the entire gait cycle whereas OpenSim cannot through the GUI itself. Through Matlab scripting plots of the heel and metatarsal position in the Z-direction were output from which the user of the code can then select which point on the graph indicates that the subject of the trial of the input dynamic file underwent heel-strike and toe-off. The point selected by the user is the time (x) point which is then converted to frame number of the normalized gait cycle. Figure 19 depicts the average of all the calculated toe-off values from each of the 3 trials of all 20 subjects from both OpenSim and Visual3D.
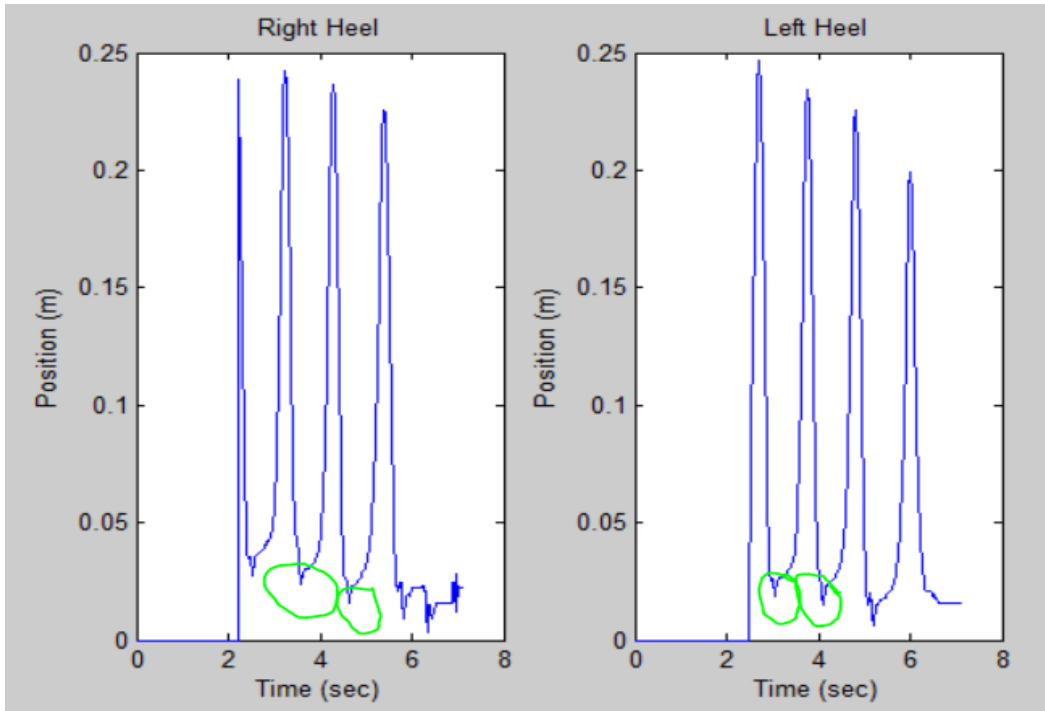
Figure 22: Heel marker plots in the Z-direction indicating the point of heel-strike.
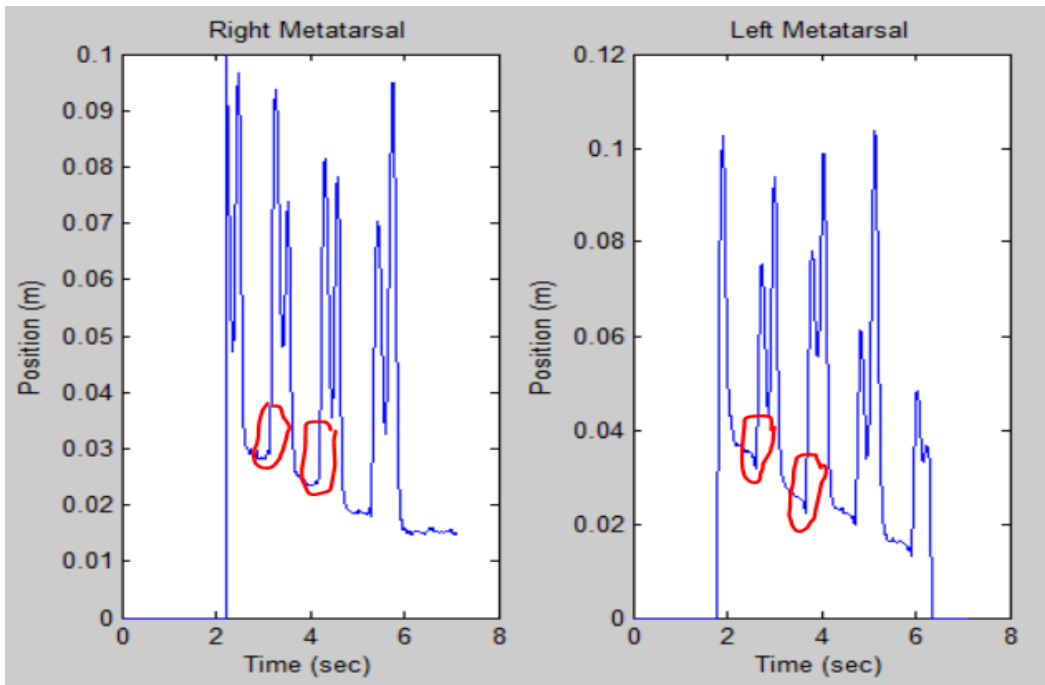
Figure 23: Metatarsal plots in the Z-direction indicating the point of toe-off.

Another difference in how the two systems output their kinematic plots is the filtering methods they use. Visual3D utilizes a 6 Hz 4th order Butterworth filter. This filter has 6 reflected samples, 6 total samples in the Buffer, and the number of bidirectional passes is 1 [9]. A 2nd order Butterworth filter with a cutoff frequency of 6/1500 was created with Matlab scripting. This filter was applied when scaling the subject data as well as calculating inverse kinematics. Although the output from both systems undergoes similar patterns, this difference in filtering may be attributed to the slight variation in kinematic output data.

Three properties need to be specified in an inverse kinematics setup file in OpenSim. This allows users to conduct the functions from OpenSim via Matlab code just so long as the appropriate setup files are specified and properly located in the respective Matlab code pathway. The three properties that need to be specified are the model to which the inverse kinematics solver is to be applied, the marker and coordinate error weightings to be used, and the specific static/dynamic trial to be used by the solver. The weighting of the each marker plays an important role in the overall kinematic output. Markers at the pelvis, knee, and ankle are typically weighted more heavily than the rest of the markers since these markers are the most accurate in calculating kinematics at their respective joints. For example, a marker on the femoral epicondyle (knee marker) has little skin/adipose tissue noise between the bone and the marker as opposed to the thigh marker which is not placed on any bony prominence. There is more muscle and adipose tissue between the hip marker and the femur. The weight of each marker is relative to one another. For example, if each marker was weighted at 1.0 as opposed to 10, the kinematic output would be the same. Visual3D does not have this feature. OpenSim can be

manipulated to give different markers more weight. Therefore the kinematic output can be changed by manipulating the weight of each marker. This very well may have played a key role in the difference in kinematic outputs from both systems.

E. Future Applications

Although this model was not statistically validated, it can be edited to fit and reciprocate the Visual3D model. OpenSim has many parameters that can be edited to produce varying results. If this model can be edited to reciprocate the Visual3D model in calculating inverse kinematics, it would be extremely beneficial. Since the muscle-length changes obtained from the sample population of subjects recruited for this study was compared to a different sample population, it is possible that the means of the muscle-length changes are statistically different. For the purposes of this experiment, the control data was assumed to be a gold standard in comparing the data from my sample population to. A gold standard of data was not able to be obtained for these specific muscles showcased in Figure 21 from existing literature.

Replacing the anterior thigh and shank markers with wand markers would improve the kinematic results. They would better capture rotational movement, especially since the anterior markers are facing skin, muscle, and adipose tissue artifact. Eliminating all joint constraints in the gait2392 model would create more degrees of freedom at the ankle. Remodeling the gait2392 model to have 3 degrees of freedom at each joint would have also improved the kinematic results.

Since OpenSim is free software, it can be implemented in more clinics across the nation. Although there are existing low-cost motion analysis capture systems available on

the market, they are still expensive (Table 1) to purchase or rent comparatively to OpenSim. The fact that OpenSim can calculate muscle-length changes during ambulation gives it reason to replace Visual3D as a motion analysis software tool. Being able to determine muscle-length changes during different points in a single gait cycle allows engineers, physicians, and clinicians to better diagnose patients with abnormal gait. Shortening or lengthening of muscles during the gait cycle is indicative of different gait abnormalities from where restorative therapies or surgical procedures can be scheduled. Aside from determining how muscles change during ambulation, OpenSim has many other features and functions, unexplored in this experiment. These features include calculating inverse dynamics, static optimization functions, reduce residuals functions, forward dynamics functions, and computed muscle control functions. All these features further expand the realm of biomechanics that can be delved into when analyzing motion and eliminate certain limitations that other biomechanical software have.

Gait analysis is important for younger and older patients alike. Abnormalities in gait can affect everyday activities and are physically limiting. Gait analysis is used to treat deficiencies in patients' limbs and other parts of the body. It allows clinicians and physicians view patients' kinematics and variation in muscle-lengths in real time and during a single gait cycle. The kinematic waveforms and changes in muscle-tendon length can be tied to each other by understanding the points of flexion/extension, ab/adduction, and internal/external rotation at each point of the gait cycle. These actions can be tied to eccentric, concentric, and isometric muscle contractions, which can help assess and justify patterns identified during gait analysis. The fact that there is instant feedback allows analysts to help create or recommend a treatment program immediately,

with the purpose being treatment that will help restore or improve any disabilities patients are incurring. Analyzing the kinematic and muscle-tendon waveforms can also tell analysts whether or not any surgical intervention is necessary, such as shortening or lengthening of any specific muscles that can improve patients' gait. The gait2392 model can be used to assess pelvis and hip kinematics best since it exhibits three degrees of freedom at both. If three degrees of freedom were exhibited at both the knee and ankle, it would give much better results at these joints since there is so much rotational and translational movement. Defining the anatomic model similar if not exactly like the conventional gait model will allow it to be used in a clinical setting for gait analysis.

IV.   CONCLUSION

OpenSim is an advanced biomechanical analysis tool with numerous features and is able to execute any programmable function through Matlab scripting. When comparing the kinematic output from OpenSim to Visual3D using the same data input, the differences vary in comparing mean maximum, minimum and range values during stance and swing phase. This disproves the original hypothesis that the kinematic output between the systems would be similar since the same function is being applied to the data, only in different software. The significant similarities between Visual3D and OpenSim kinematic output and spatiotemporal parameters are summarized in Tables 10 and 11, respectively. With many different parameters that can be edited and manipulated in OpenSim through XML files and Matlab scripting, OpenSim is able to output varying kinematics relative to these parameters.

Table 10: Summary table of kinematic comparison showing significant similarities.

Gait Cycle	Kinematics		
	Left	Right	Pelvis
Stance	Min Knee Angle	Max Hip Flex/Ext	Range Pelvic Tilt
		Max Hip Ab/Adduction	Max Pelvic Obl
		Min Knee Angle	Range Pelvic Rot
Swing	Max Hip Flex/Ext	Max Hip Flex/Ext	Range Pelvic Tilt
	Min Hip Ab/Adduction	Max Knee Angle	Range Pelvic Obl
	Range Knee Angle		Range Pelvic Rot

Table 11: Summary table of spatiotemporal parameter comparison.

Spatiotemporal Parameters
Stride Length
Right Cadence
Left Cadence
Walking Speed

The weighting of markers in OpenSim, the difference in filtering methods, difference in selection of heel-strike and toe-off between systems, and the lack of wands all contributed to differences in kinematic output between the software. To augment the accuracy of the gait2392 model, these parameters should be identical to the parameters in the software OpenSim is being compared with, whether it is Visual3D or any other biomechanical modeling software. Being able to determine muscle-length changes during ambulation is a key feature OpenSim has in assessing motion analysis which sets it apart from Visual3D. Significant similarities between the experimental and control data are highlighted in Tables 7 and 8. The scarcity in similarities supports the original hypothesis that there may be differences in muscle-tendon lengths between the data since they are

from different sample populations. Although Visual3D has many biomechanical analysis tools, OpenSim's muscle analysis tool provides a further, more in-depth analysis of gait, which can be utilized by clinicians, physicians, and biomedical engineers to highlight abnormalities and assign any further restorative therapies or surgeries if needed.

BIBLIOGRAPHY

1. Chleboun, G.S., et al., Fascicle length change of the human tibialis anterior and vastus lateralis during walking. J Orthop Sports Phys Ther, 2007. 37(7): p. 372-9.

2. Feng, J., et al., *Applications of gait analysis in pediatric orthopaedics.* Current Orthopaedic Practice, 2016. 27(4): p. 455-464.

3. Khouri, N. and E. Desailly, *Contribution of clinical gait analysis to single-event multi-level surgery in children with cerebral palsy.* Orthop Traumatol Surg Res, 2017. 103(1s): p. S105-s111.

4. Mehling, M., *Implementation of a Low Cost Marker Based Infrared Light Optical Tracking System.* 2006.

5. Chidlren, S.H.f., *Milwaukee Foot Model.*

6. Kidder, S.M., et al., *A system for the analysis of foot and ankle kinematics during gait.* IEEE Trans Rehabil Eng, 1996. 4(1): p. 25-32.

7. Kainz, H., et al., *Reliability of four models for clinical gait analysis.* Gait Posture, 2017. 54: p. 325-331.

8. Baker, R., *Gait analysis methods in rehabilitation.* J Neuroeng Rehabil, 2006. 3: p. 4.

9. Kertis, J.D., *Biomechanical Evaluation of an Optical System for Quantitative Human Motion Analysis.* 2012.

10. Baker, R., L. Finney, and J. Orr, *A new approach to determine the hip rotation profile from clinical gait analysis data.* Human Movement Science, 1999. 18(5): p. 655-667.

11. Moissenet, F., L. Cheze, and R. Dumas, *A 3D lower limb musculoskeletal model for simultaneous estimation of musculo-tendon, joint contact, ligament and bone forces during gait.* J Biomech, 2014. 47(1): p. 50-8.

12. Lathrop-Lambach, R.L., et al., *Evidence for joint moment asymmetry in healthy populations during gait.* Gait Posture, 2014. 40(4): p. 526-31.

13. Gigi, R., et al., *Deviations in gait metrics in patients with chronic ankle instability: a case control study.* J Foot Ankle Res, 2015. 8(1): p. 1.

14. NYC, M.C. *How much does motion capture cost?* ;
    http://www.motioncapturenyc.com/cost/].

15. Simon, S.R., *Quantification of human motion: gait analysis—benefits and limitations to its application to clinical problems.* Journal of Biomechanics, 2004. 37(12): p. 1869-1880.

16. Pearsall, D.J. and P.A. Costigan, *The effect of segment parameter error on gait analysis results.* Gait Posture, 1999. 9(3): p. 173-83.

17. Stagni, R., et al., *Effects of hip joint centre mislocation on gait analysis results*. Vol. 33. 2000. 1479-87.

18. Biomechanics, C.-M.R. *Visual3D v6 Professional*. http://www2.c-motion.com/products/visual3d].

19. SimTK. *License for OpenSim 3.0 and Later*. https://simtk-confluence.stanford.edu/display/OpenSim/License+for+OpenSim+3.0+and+Later].

20. Motion, C. *Wands For Gait*. http://codamotion.com/index.php/applications/hardware/item/68-wands-for-gait].

21. Martín-Félez R., M.R.A., Sánchez J.S. , *Human Recognition Based on Gait Poses. In: Vitrià J., Sanches J.M., Hernández M. (eds) Pattern Recognition and Image Analysis.* 2011. Lecture Notes in Computer Science, vol 6669. Springer, Berlin, Heidelberg.

22. Barre, A. and S. Armand, *Biomechanical ToolKit: Open-source framework to visualize and process biomechanical data.* Comput Methods Programs Biomed, 2014. 114(1): p. 80-7.

23. Mantoan, A., et al., *MOtoNMS: A MATLAB toolbox to process motion data for neuromusculoskeletal modeling and simulation*. Vol. 10. 2015. 12.

24. Arnold, E.M. and S.L. Delp, *Fibre operating lengths of human lower limb muscles during walking.* Philosophical Transactions of the Royal Society B: Biological Sciences, 2011. 366(1570): p. 1530-1539.

25 Corkery, M., et al., *Establishing normal values for lower extremity muscle length in college-age students.* Physical Therapy in Sport, 2007. 8(2): p. 66-74.

26. Parikh, C. and M. Arora, *Establishing Normal Values for Lower Extremity Muscle Length and comparison of muscle length from dominant to non dominant side in Elite Cricketers aged 15-22 years*. Vol. 4. 2015. 1.

27. van der Krogt, M.M., C.A.M. Doorenbosch, and J. Harlaar, *Muscle length and lengthening velocity in voluntary crouch gait.* Gait & Posture, 2007. 26(4): p. 532-538.

28. Rao, S., F. Dietz, and H.J. Yack, *Estimates of gastrocnemius muscle length during simulated pathological gait.* J Appl Biomech, 2013. 29(2): p. 127-34.

29. Singh, D.A.P. *Bone Spine - Normal Gait Cycle*. http://boneandspine.com/normal-gait-cycle/].

30. Beardsley, C., *Pelvic Tilt.*

31. Kainz, H., et al., *Joint kinematic calculation based on clinical direct kinematic versus inverse kinematic gait models.* Journal of Biomechanics, 2016. 49(9): p. 1658-1669.

32. Delp, S.L., et al., *OpenSim: Open-Source Software to Create and Analyze Dynamic Simulations of Movement.* IEEE Transactions on Biomedical Engineering, 2007. 54(11): p. 1940-1950.

33. Lathrop-Lambach, R., A. Chaudhari, and R. Siston, *Comparative Assessment of Bone Pose Estimation Using Point Cluster Technique and OpenSim*. Vol. 133. 2011. 114503.
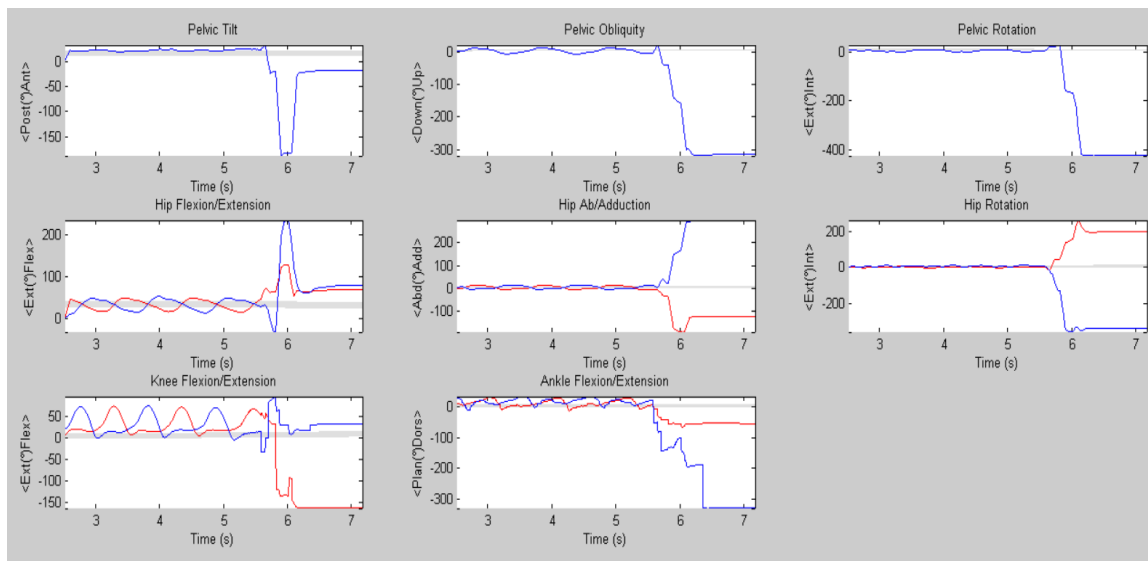
Figure 24: Lower-extremity kinematic plot in real time for one full dynamic trial.
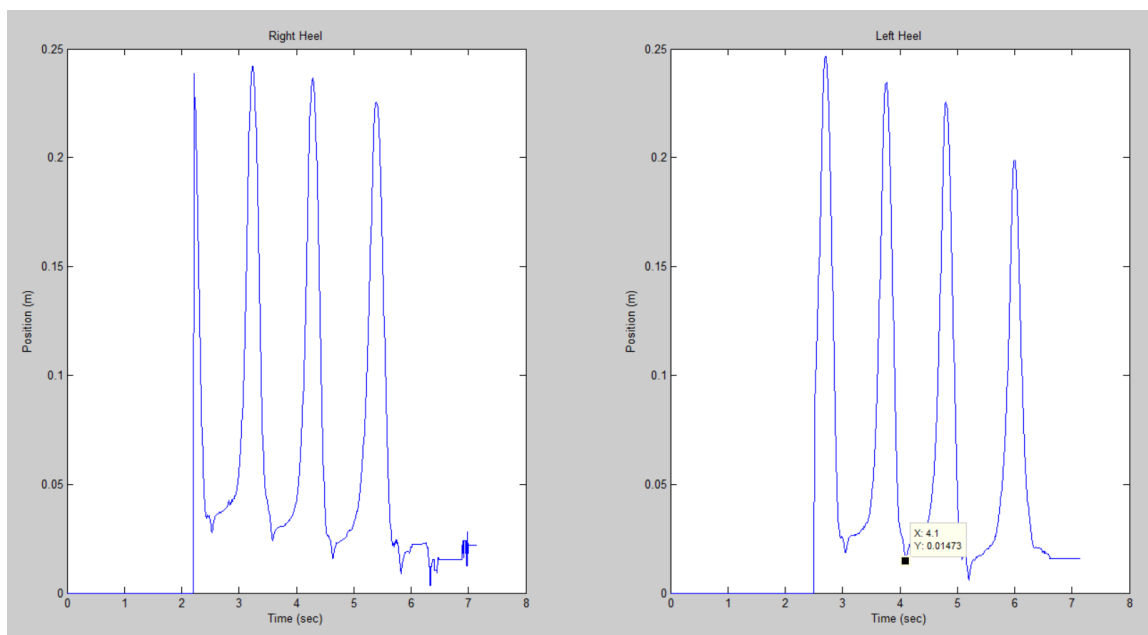
Figure 25: Heel marker plot asking user to select point of heel-strike.
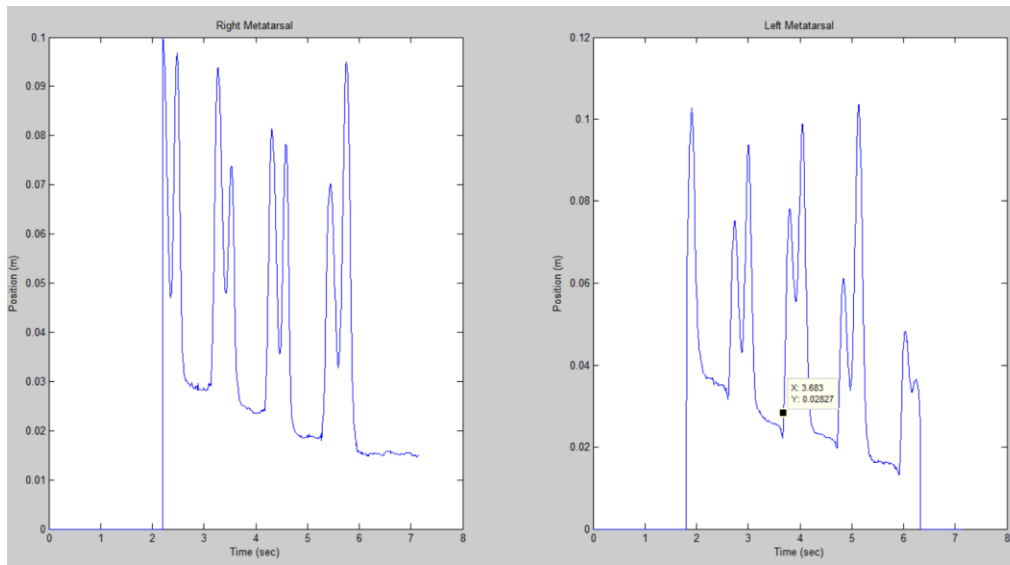
Figure 26: Metatarsal marker plot asking user to select point of toe-off.

```
IK compute time = 10959ms
What is the first minimum value of the Right Heel Plot?2.533
What frame number matches up with this value?3
What is the second minimum value of the Right Heel Plot?3.583
What frame number matches up with this value?129
What is the first minimum value of the Left Heel Plot?3.058
What frame number matches up with this value?66
What is the second minimum value of the Left Heel Plot?4.1
What frame number matches up with this value?191
What is the first minimum value of the Right Meta Plot?3.15
What is the first minimum value of the Left Meta Plot?3.683

stride_length =

    1.2199


R_cadence =

  114.2857


L_cadence =

  116.0542


speed =

    1.1744
```

Figure 27: Matlab user-interface and spatiotemporal results in the Command Window.
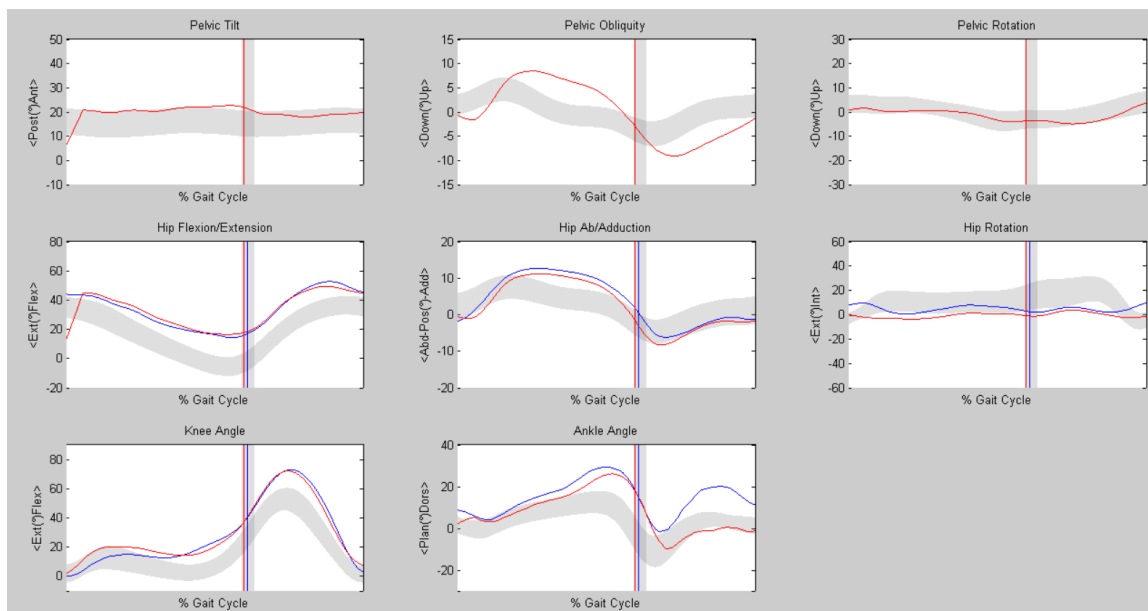
Figure 28: Final output from OpenSim/Matlab code for inverse kinematics.

APPENDIX B
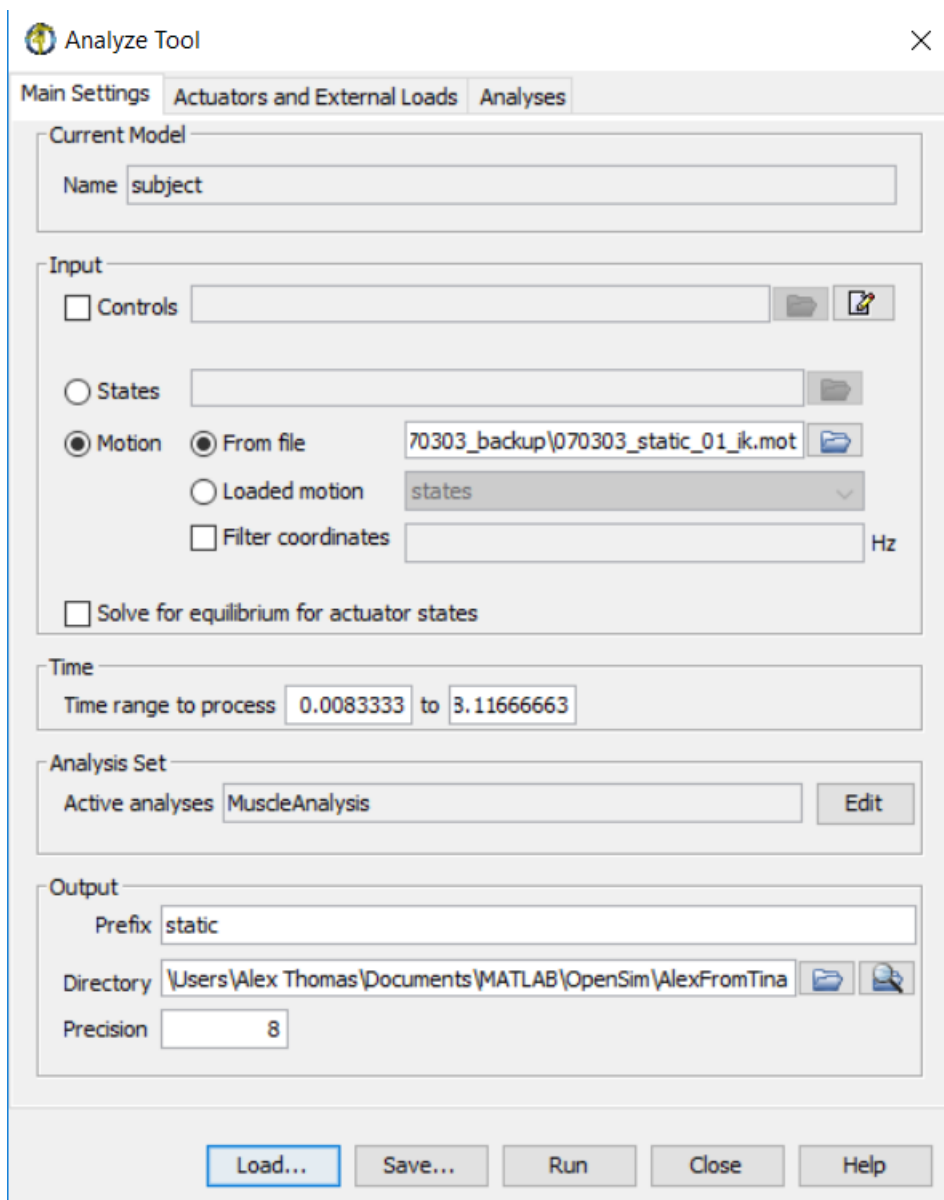
Figure 29: OpenSim graphical user-interface when conducting muscle analysis where static and dynamic files must be input.
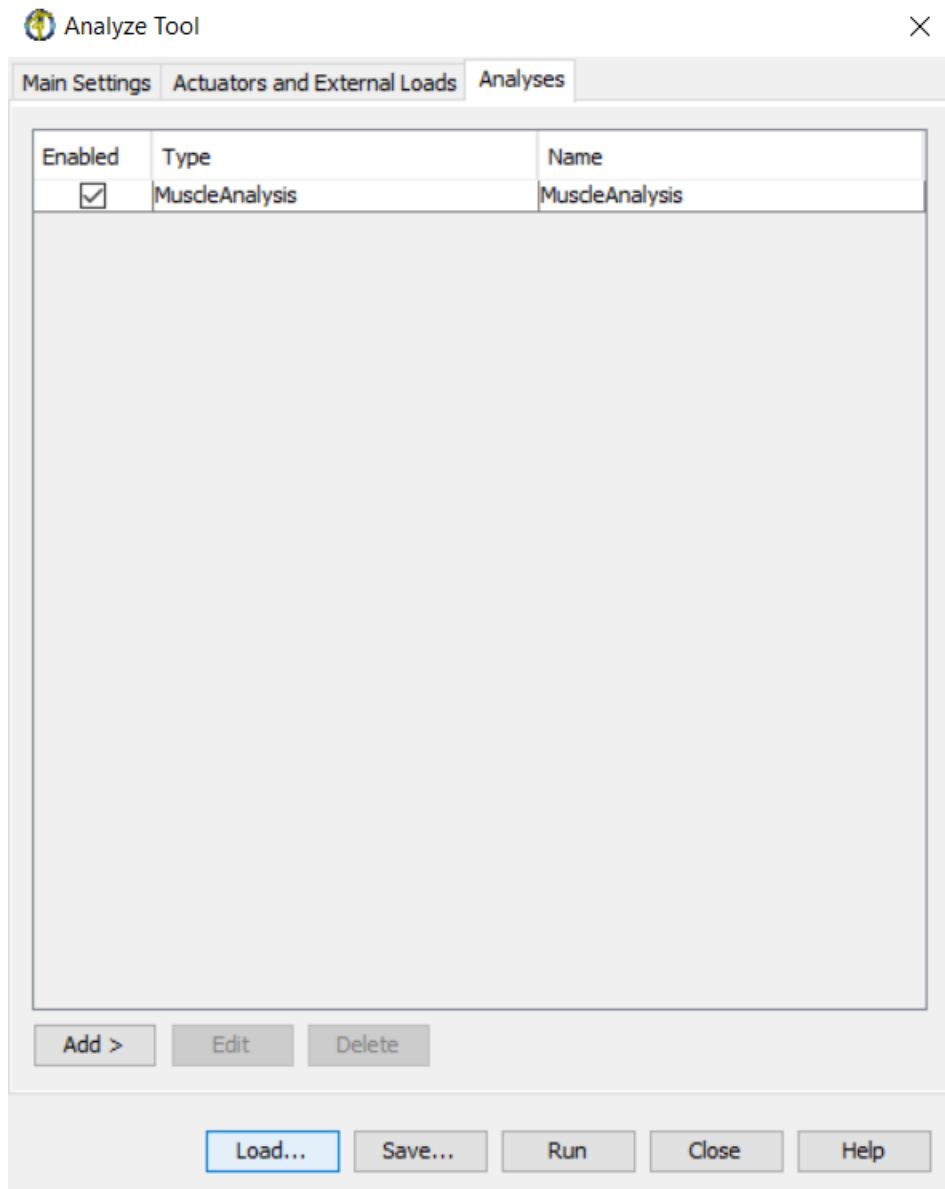
Figure 30: OpenSim GUI Analyses tab where Muscle Analysis is selected to determine muscle-length changes.
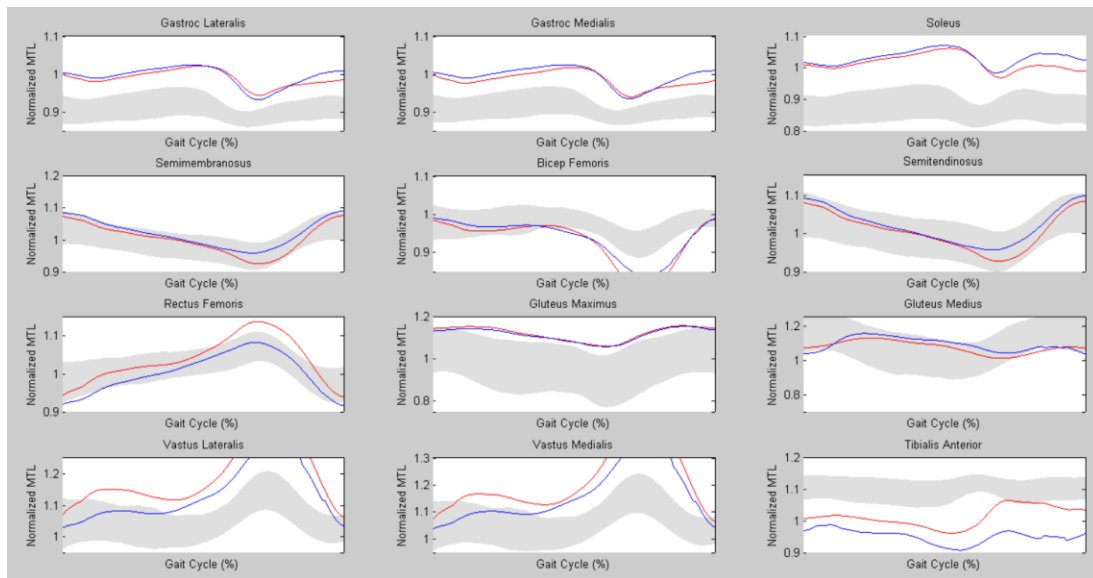
Figure 31: Final output from OpenSim/Matlab code for muscle-length variation.

Table 12: Statistical comparison of the gastroc lateralis during stance phase.

			Gastroc Lateralis		
			Experimental Mean	Control Mean	P-Value
Stance	Right	Maximum	1.00852	0.93447	0
		Minimum	0.95935	0.891679	0
		Range	0.04917	0.0427901	0
	Left	Maximum	1.01204	0.921581	0
		Minimum	0.95605	0.88963	0
		Range	0.05599	0.0319509	0

Table 13: Statistical comparison of the gastroc medialis during stance phase.

			Gastroc Medialis		
			Experimental Mean	Control Mean	P-Value
Stance	Right	Maximum	1.00803	0.936668	0
		Minimum	0.95841	0.895274	0
		Range	0.04962	0.0413938	0
	Left	Maximum	1.01341	0.924444	0
		Minimum	0.95893	0.893606	0
		Range	0.05448	0.0308402	0

Table 14: Statistical comparison of the soleus during stance phase.

			Soleus		
			Experimental Mean	Control Mean	P-Value
Stance	Right	Maximum	1.02728	0.901921	0
		Minimum	0.96173	0.850168	0
		Range	0.06555	0.0517528	0
	Left	Maximum	1.02686	0.883499	0
		Minimum	0.96249	0.850492	0
		Range	0.06437	0.0330074	0

Table 15: Statistical comparison of the semimembranosus during stance phase.

			Semimembranosus		
			Experimental Mean	Control Mean	P-Value
Stance	Right	Maximum	1.052	1.04115	0.004
		Minimum	0.92912	0.956198	0
		Range	0.12288	0.0849558	0
	Left	Maximum	1.05508	1.03405	0
		Minimum	0.93968	0.968055	0
		Range	0.11541	0.0659914	0

Table 16: Statistical comparison of the bicep femoris during stance phase.

			Bicep Femoris		
			Experimental Mean	Control Mean	P-Value
Stance	Right	Maximum	0.99695	0.992133	0.059
		Minimum	0.92702	0.967088	0
		Range	0.06994	0.0250455	0
	Left	Maximum	1.00001	0.990327	0.042
		Minimum	0.93938	0.96812	0
		Range	0.06063	0.022207	0

Table 17: Statistical comparison of the semitendinosis during stance phase.

			Semitendinosis		
			Experimental Mean	Control Mean	P-Value
Stance	Right	Maximum	1.05649	1.04938	0.054
		Minimum	0.92803	0.962266	0
		Range	0.12847	0.0871168	0
	Left	Maximum	1.05875	1.04314	0
		Minimum	0.93527	0.976823	0
		Range	0.12348	0.0663128	0

Table 18: Statistical comparison of the rectus femoris during stance phase.

			Rectus Femoris		
			Control Mean	P-Value	Experimental Mean
Stance	Right	Maximum	1.04938	0.054	1.11137
		Minimum	0.962266	0	0.95294
		Range	0.0871168	0	0.15843
	Left	Maximum	1.04314	0	1.08413
		Minimum	0.976823	0	0.94974
		Range	0.0663128	0	0.13439

Table 19: Statistical comparison of the gluteus maximus during stance phase.

			Gluteus Maximus		
			Experimental Mean	Control Mean	P-Value
Stance	Right	Maximum	1.09249	1.05885	0
		Minimum	0.96507	0.908806	0
		Range	0.12743	0.150043	0.002
	Left	Maximum	1.0872	1.02992	0
		Minimum	0.96566	0.884886	0
		Range	0.12155	0.145036	0.002

Table 20: Statistical analysis of the gluteus medius during stance phase.

			Gluteus Medius		
			Experimental Mean	Control Mean	P-Value
Stance	Right	Maximum	1.09249	1.09189	0.914
		Minimum	0.96507	0.922139	0
		Range	0.12743	0.169752	0
	Left	Maximum	1.0872	1.06691	0.002
		Minimum	0.96566	0.863886	0
		Range	0.12155	0.203022	0

Table 21: Statistical analysis of the vastus lateralis during stance phase.

			Vastus Lateralis		
			Experimental Mean	Control Mean	P-Value
Stance	Right	Maximum	1.1824	1.06675	0
		Minimum	1.01151	1.01466	0.727
		Range	0.17088	0.0520916	0
	Left	Maximum	1.132	1.06562	0
		Minimum	1.00789	1.01839	0.277
		Range	0.12415	0.0472293	0

Table 22: Statistical analysis of the vastus medialis during stance phase.

			Vastus Medialis		
			Experimental Mean	Control Mean	P-Value
Stance	Right	Maximum	1.20765	1.07893	0
		Minimum	1.01226	1.0165	0.66
		Range	0.19539	0.0624284	0
	Left	Maximum	1.1552	1.07745	0
		Minimum	1.0111	1.02107	0.382
		Range	0.14412	0.0563833	0

Table 23: Statistical analysis of the tibialis anterior during stance phase.

			Tibialis Anterior		
			Experimental Mean	Control Mean	P-Value
Stance	Right	Maximum	1.02722	1.11497	0
		Minimum	0.97506	1.07652	0
		Range	0.05217	0.0384463	0
	Left	Maximum	1.02308	1.11682	0
		Minimum	0.94915	1.09132	0
		Range	0.07393	0.0254927	0

Table 24: Statistical analysis of the gastroc lateralis during swing phase.

			Gastroc Lateralis		
			Experimental Mean	Control Mean	P-Value
Swing	Right	Maximum	0.98976	0.916638	0
		Minimum	0.91586	0.881379	0
		Range	0.0739	0.0352596	0
	Left	Maximum	0.99173	0.907935	0
		Minimum	0.90334	0.879029	0
		Range	0.08839	0.0289058	0

Table 25: Statistical analysis of the gastroc medialis during swing phase.

			Gastroc Medialis		
			Experimental Mean	Control Mean	P-Value
Swing	Right	Maximum	0.98984	0.919429	0
		Minimum	0.91655	0.885177	0
		Range	0.07329	0.0342518	0
	Left	Maximum	0.99261	0.911351	0
		Minimum	0.90673	0.883062	0
		Range	0.08588	0.0282894	0

Table 26: Statistical analysis of the soleus during swing phase.

			Soleus		
			Experimental Mean	Control Mean	P-Value
Swing	Right	Maximum	0.99504	0.890073	0
		Minimum	0.92175	0.84361	0
		Range	0.0733	0.0464628	0
	Left	Maximum	1.00601	0.876753	0
		Minimum	0.92184	0.848993	0
		Range	0.08418	0.0277595	0

Table 27: Statistical analysis of the semimembranosus during swing phase.

			Semimembranosus		
			Experimental Mean	Control Mean	P-Value
Swing	Right	Maximum	1.05898	1.04227	0
		Minimum	0.90876	0.94098	0
		Range	0.15022	0.101295	0
	Left	Maximum	1.06033	1.04387	0
		Minimum	0.93147	0.95451	0
		Range	0.12886	0.089357	0

Table 28: Statistical analysis of the bicep femoris during swing phase.

			Bicep Femoris		
			Experimental Mean	Control Mean	P-Value
Swing	Right	Maximum	1.00477	0.989683	0
		Minimum	0.83138	0.916167	0
		Range	0.17339	0.0735169	0
	Left	Maximum	1.0051	0.988069	0.001
		Minimum	0.86587	0.927143	0
		Range	0.13923	0.0609256	0

Table 29: Statistical analysis of the semitendinosis during swing phase.

			Semitendinosis		
			Experimental Mean	Control Mean	P-Value
Swing	Right	Maximum	1.06422	1.04925	0
		Minimum	0.90946	0.943994	0
		Range	0.15476	0.105261	0
	Left	Maximum	1.06507	1.0532	0.003
		Minimum	0.92727	0.959755	0
		Range	0.13779	0.0934472	0

Table 30: Statistical analysis of the rectus femoris during swing phase.

			Rectus Femoris		
			Experimental Mean	Control Mean	P-Value
Swing	Right	Maximum	1.1436	1.07845	0
		Minimum	0.9369	0.969844	0
		Range	0.20671	0.108607	0
	Left	Maximum	1.10449	1.06433	0
		Minimum	0.94118	0.968532	0
		Range	0.16331	0.0957962	0

Table 31: Statistical analysis of the gluteus maximus during swing phase.

			Gluteus Maximus		
			Experimental Mean	Control Mean	P-Value
Swing	Right	Maximum	1.09123	1.04814	0
		Minimum	0.96969	0.903079	0
		Range	0.12154	0.145063	0.001
	Left	Maximum	1.08781	1.03462	0
		Minimum	0.96825	0.88409	0
		Range	0.11956	0.150534	0

Table 32: Statistical analysis of the gluteus medius during swing phase.

			Gluteus Medius		
			Experimental Mean	Control Mean	P-Value
Swing	Right	Maximum	1.09123	1.08639	0.338
		Minimum	0.96969	0.940789	0
		Range	0.12154	0.145602	0.001
	Left	Maximum	1.08781	1.08034	0.175
		Minimum	0.96825	0.878528	0
		Range	0.11956	0.20181	0

Table 33: Statistical analysis of the vastus lateralis during swing phase.

			Vastus Lateralis		
			Experimental Mean	Control Mean	P-Value
Swing	Right	Maximum	1.3157	1.15333	0
		Minimum	0.98122	1.02146	0.001
		Range	0.33447	0.131867	0
	Left	Maximum	1.2516	1.13705	0
		Minimum	0.9949	1.02454	0.007
		Range	0.25665	0.112509	0

Table 34: Statistical analysis of the vastus medialis during swing phase.

			Vastus Medialis		
			Experimental Mean	Control Mean	P-Value
Swing	Right	Maximum	1.3705	1.17713	0
		Minimum	0.981	1.02544	0
		Range	3895	0.15169	0
	Left	Maximum	1.2932	1.15825	0
		Minimum	0.9945	1.02893	0.008
		Range	0.29873	0.129315	0

Table 35: Statistical analysis of the tibialis anterior during swing phase.

			Tibialis Anterior		
			Experimental Mean	Control Mean	P-Value
Swing	Right	Maximum	1.05409	1.11972	0
		Minimum	1.00153	1.08541	0
		Range	0.05256	0.034315	0
	Left	Maximum	1.0239	1.11797	0
		Minimum	0.97392	1.09663	0
		Range	0.04999	0.0213401	0